REPORT DOCUMENTATION PAGE

Form Approved

AFRL-SR-AR-TR-08-0062

1. REPORT DATE (DD-MM-YYYY)	2. REPORT TYPE	3. DATES COVERED (From - To)
	Final Technical Report	15 February 2004 – 15 August 2007

4. TITLE AND SUBTITLE
Time-Frequency Filtering and Carrier-Phase Ambiguity Resolution for GPS-Based TSPI Systems in Jamming Environment

5a. CONTRACT NUMBER

5b. GRANT NUMBER
FA9550-04-1-0115

5c. PROGRAM ELEMENT NUMBER

6. AUTHOR(S)
Professor Ying-Cheng Lai

5d. PROJECT NUMBER

5e. TASK NUMBER

5f. WORK UNIT NUMBER

7. PERFORMING ORGANIZATION NAME(S) AND ADDRESS(ES)
Mathematics & Statistics
Arizona State University
P.O. Box 871804
Temple AZ 85287

8. PERFORMING ORGANIZATION REPORT NUMBER

9. SPONSORING/MONITORING AGENCY NAME(S) AND ADDRESS(ES)
USAF/AFRL
AFOSR
875 North Randolph Street
Arlington VA 22203
Dr Neal Glassman/NL

10. SPONSOR/MONITOR'S ACRONYM(S)
AFOSR

11. SPONSORING/MONITORING AGENCY REPORT NUMBER
N/A

12. DISTRIBUTION AVAILABILITY STATEMENT

Distribution Statement A: Approved for public release. Distribution is unlimited.

13. SUPPLEMENTARY NOTES

14. ABSTRACT

In the project period, we developed a class of time-frequency filters based on the combination of the empirical-mode decomposition (EMD) method and a general blind-source separation (BSS) algorithm. We obtained evidence that the method is able to separate jamming from the GPS signal for JSR up to 45dB.

A forefront research area in signal processing is particle filters. The idea is to evolve the probability distribution of a signal by using a large number of particles according to the system equations and some stochastic processes, which is similar to Monte-Carlo simulation in physics and chemistry. Motivated by the fact that particle filters have been used widely in various types of signal-processing tasks, we applied this technique to GPS positioning of moving objects in a jamming environment. In particular, we considered a class of regularized particle filters, suitable for estimating the position of a moving object (e.g., a car) equipped with some proper GPS C/A code receiver. Theoretically, a question of interest is how the estimation error depends on uncertainties in the velocity measurement of the car and on the noise level in the GPS signal. Our analysis of the covariance matrix constructed from simulated particles led to a formula relating this matrix to the covariance matrices of the velocity and of the position error from least-squares processing of GPS pseudoranges. The formula was verified by numerical simulations.

15. SUBJECT TERMS

16. SECURITY CLASSIFICATION OF:			17. LIMITATION OF ABSTRACT	18. NUMBER OF PAGES	19a. NAME OF RESPONSIBLE PERSON
a. REPORT	b. ABSTRACT	c. THIS PAGE	Unclassified	32	19b. TELEPONE NUMBER (Include area code)

Final Report

This report summarizes activities under the Air Force Office of Scientific Research (AFOSR) Grant No. FA9550-04-1-0115 entitled "Time-frequency filtering and carrier-phase ambiguity resolution for GPS-based TSPI systems in jamming environment." The duration of the project is 2/16/2004 to 8/15/2007. The report is divided into the following Sections:

1. Objectives
2. Description of Achievements of Objectives
3. New Findings
4. Personnel Supported and Theses Supervised by PI
5. List of Publications
6. Interactions/Transitions
7. Past Honors

1 Objectives

1. Time-frequency filtering of jammed GPS signals;
2. Carrier-phase ambiguity resolution in the presence of noise.

2 Description of Achievements of Objectives

Both Objectives have been accomplished. Results have been published in two refereed-journal papers and two refereed conference-proceeding papers. Two final papers are being prepared for submission.

2.1 Time-frequency filtering of jammed GPS signals

For Test and Evaluation (T&E) systems on DOD test ranges, GPS has been used as the primary source of Time-Space-Position Information (TSPI). The accuracy requirement for TSPI is in the sub-meter range, an order of magnitude higher than that required for actual combat systems. To achieve the high accuracy, it is necessary to use carrier-phase tracking of GPS signals. To emulate the characteristics of enemy GPS threats in the battlefield, the TSPI test environment also includes GPS jamming sources.

The spread-spectrum structure of GPS signals provides inherent jamming tolerance for GPS receivers. After despreading the received signal, the original satellite signals are collapsed into a narrow band around the carrier frequency, while the jamming signals are spread due to the lack of correlation with the PN codes that encode the satellite information. The portion of the spread jamming signal remaining within the frequency band of the tracking loop enters the loop together with the satellite signal. Thus signal tracking can be stable only if the jamming-to-signal ratio (JSR) is below the processing gain of the spreading code. In general, a JSR of greater than 40dB will prevent the GPS receiver from tracking the satellite signals and estimating its own position. In a hostile environment where jamming sites may be close to GPS users, a larger JSR is possible. How to achieve the desired accuracy for a GPS-based TSPI system in the presence of strong jamming is an important but outstanding problem.

In the project period, we developed a class of time-frequency filters based on the combination of the empirical-mode decomposition (EMD) method and a general blind-source separation (BSS) algorithm. We obtained evidence that the method is able to separate jamming from the GPS signal for JSR up to 45dB.

A forefront research area in signal processing is particle filters. The idea is to evolve the probability distribution of a signal by using a large number of particles according to the system equations and some stochastic processes, which is similar to Monte-Carlo simulation in physics and chemistry. Motivated by the fact that particle filters have been used widely in various types of signal-processing tasks, we applied this technique to GPS positioning of moving objects in a jamming environment. In particular, we considered a class of regularized particle filters, suitable for estimating the position of a moving object (e.g., a car) equipped with some proper GPS C/A code receiver. Theoretically, a question of interest is how the estimation error depends on uncertainties in the velocity measurement of the car and on the noise level in the GPS signal. Our analysis of the covariance matrix constructed from simulated particles led to a formula relating this matrix to the covariance matrices of the velocity and of the position error from least-squares processing of GPS pseudoranges. The formula was verified by numerical simulations.

Practically, in order to address the problem of occasional but inevitable large errors (outliers) in the GPS observations, we developed a robust particle-filtering technique. We demonstrated that the strategy is effective for mitigating the effect of outliers for both Gaussian and non-Gaussian noise sources. Even in the absence of outliers, our strategy can be useful for improving the positioning accuracy.

Publications

- V. Kamath, Y.-C. Lai, S. Urval, and L. Zhu, "Empirical mode decomposition and blind source separation methods for antijamming with GPS signals," pp. 335-341 in IEEE PLANS (Position Location and Navigation Symposium), April 24-26, 2006, San Diego, CA.
- L. Huang and Y.-C. Lai, "Sequential Monte Carlo scheme for Bayesian estimation in the presence of data outliers," *Physical Review E* **75**, 056705(1-6) (2007).
- V. Kamath and Y.-C. Lai, "Empirical mode decomposition with applications to noise reduction and antijamming," in preparation.

2.2 Carrier-phase ambiguity resolution in the presence of noise

In order to determine a GPS receiver's position, the following two pieces of information are needed: (1) the satellite positions and (2) the traveling times of signals or the numbers of wavelength. With these, the receiver's position can be calculated by a simple trilateration procedure.

Information about the satellite positions is encoded in the GPS signal via the traditional spread-spectrum method. The respective distances between satellites and the GPS receiver can be obtained by figuring out the numbers of wavelengths of the carrier signals. The fractional parts of the wavelength can be measured by phase-locked loop based detectors embedded in the receiver. The integer parts are ambiguous and these integer ambiguities must be resolved accurately to meet the T&E requirement of sub-meter precision in a jamming environment. There exist several integer-parameter estimation methods, but how they perform under strong, non-Gaussian noise or jamming is unknown. During the project period, we evaluated the performance of a state-of-art integer-parameter estimation algorithm and explored improvements for use in a jamming environment.

Particle filters are naturally suitable for integer-parameter estimation with GPS carrier waves, as the system equations can be obtained via straightforward geometrical arguments. During the project period we successfully demonstrated the feasibility of this approach.

Publications

- M. Shah and Y.-C. Lai, "Performance of integer parameter estimation algorithm for GPS signals in noisy environment," pp. 166-174 in *ION GNSS 17th International Technical Meeting of the Satellite Division*, Sept. 21-24, 2004, Long Beach, CA.
- L. Zhu, Y.-C. Lai, M. Shah, and S. Mahmood "Efficiency of carrier-phase integer ambiguity resolution for precise GPS positioning in noisy environments," *Journal of Geodesy* **81**, 149-156 (2007).
- A. Rammohan, L. Huang, and Y.-C. Lai, "Integer ambiguity resolution using particle filters," in preparation.

3 New Findings

3.1 Performance of integer least-squares method for ambiguity resolution with GPS signals in the presence of noise

3.1.1 Background

In general, centimeter GPS positioning accuracy requires a precise tracking of the carrier phase that consists of two parts: a directly measured fractional part (with measurement error at millimeter level) and an unknown integer part, also called the *integer ambiguity*. The key to carrier-phase-based precise positioning is to resolve the integer ambiguity, which is an extremely challenging task, particularly when large noise or jamming is present.

Existing ambiguity resolution techniques can be divided into several categories [1]. The first category includes the simplest techniques which use C/A-code or P-code pseudoranges directly to determine the ambiguities of the corresponding carrier phase observations. The precision of the code range is not good enough to determine the integer ambiguities and inter frequency linear combinations are usually used for estimating ambiguities [2]. The second category of algorithms employ the Ambiguity Function Method (AFM) [3]. This technique uses only the fractional value of the instantaneous carrier-phase measurement and, hence, the ambiguity function values are not affected by the whole cycle change of the carrier phase or by cycle slips (also see [2, 4]). The third category comprises the most abundant group of techniques which are based on the theory of integer least squares [5, 6, 7, 8, 9, 10, 11, 12, 13, 14, 15, 16, 17, 18]. Parameter estimation in theory is carried out in three steps: float solution, integer-ambiguity estimation, and fixed solution. Each technique makes use of the variance-covariance matrix obtained at the float solution step and employs different ambiguity search processes at the integer ambiguity estimation step. Based on certain search criterion [19], the search algorithm can utilize the traditional techniques of mathematical programming to guide the global optimization [20, 12, 13] and/or decorrelation techniques to reduce the search space [9, 16, 14]. Guided random searching techniques can be used to combat nonlinearity [21, 17]. Note, however, that decorrelation would help speed up searching for the integer solution only if the dimension is not too large [14].

For any method, a practical concern (especially for kinematic positioning) is that the resolution time of the integer ambiguity is sensitive to the carrier-phase measurement noise. In a noisy environment, e.g., battle field with strong jamming signals, radio frequency interference (RFI) signals are spread in the frequency domain by the de-spreading process. These spectrally spread RFIs increase the effective noise floor in a GPS receiver, making carrier-phase measurements more noisy and hence the time to resolve integer ambiguity longer. Whenever a loss of track due to jamming or blockade occurs, the integer ambiguity has to be resolved again, during which no high-precision position information can be available. To reduce the phase-measurement noise and the integer-ambiguity resolution time, various techniques such as those based on signal processing (e.g., time-frequency domain processing) [22], subspace processing [23] and/or receiver antenna design (e.g., beam forming, null steering) have been proposed [24, 25] for antijamming. However, even with the application of these techniques, typically there are still residual errors in the phase measurement and greater efforts are required for fast resolution of the integer ambiguity. Given a minimal requirement for positioning accuracy and acquisition time, it is desirable to know the corresponding noise level of carrier-phase measurements, in order to employ only the necessary jamming mitigation techniques.

During the project period, we investigated the performance of a typical integer least-squares ambiguity resolution algorithm in noisy environments. In particular, we addressed how the convergence (acquisition) time of the algorithm depends on the carrier-phase measurement noise. Naively, one may expect that the time and the noise variance σ^2 have a linear relationship, as suggested by the fact that the variance of n independent noisy measurements of variance σ^2 is σ^2/n. However, our theoretical analysis showed that the acquisition time depends linearly on the standard deviation of noise (or the noise amplitude) σ, not on σ^2, as also verified by numerical simulations using a generic integer-parameter estimation algorithm [16]. Since the naive relationship $n \propto \sigma^2$ would require much more observation samples than the linear relation $n \propto \sigma$ (for large σ and n), the finding is important for the design of precise GPS positioning system in noisy environments with tight constraint on time, such as in kinematic GPS positioning. Our finding is particularly encouraging as it suggests the possibility of having integer-parameter estimator to achieve significantly short convergence time for precise positioning.

In the following, we briefly review a standard GPS model and describe a generic ambiguity resolution algorithm based on integer least squares. Our focus is on the performance of the algorithm in the presence of noise. We shall also derive a theoretical relationship between the convergence time and the noise amplitude and provide numerical verification.

3.1.2 System model

GPS signals are usually corrupted by jamming and several other forms of errors. These error sources can be partially cancelled by using the technique of double-differencing. For positioning based on the carrier phase, we assume that jamming and the residual errors can be modeled as noise in the phase. Under this consideration, the distance between a satellite i and a receiver A can be modeled as

$$\rho_A^i(k) = \lambda[\Phi_A^i(k) + n_A^i] + v(k), \tag{1}$$

where k is the discrete sampling time, λ is the wavelength of the carrier, Φ is the fractional part of the carrier phase, n is the integer part of the initial carrier phase (i.e., at $k = 0$), and v is the modeling error. The range ρ can be expressed in terms of the satellite position $[x^i(k), y^i(k), z^i(k)]$ and receiver position $[x_A(k), y_A(k), z_A(k)]$:

$$\rho_A^i(k) = \{[x^i(k) - x_A(k)]^2 + [y^i(k) - y_A(k)]^2 + [z^i(k) - z_A(k)]^2\}^{1/2}. \tag{2}$$

The goal is to calculate the receiver position $[x_A(k), y_A(k), z_A(k)]$ by using known positions of at least three satellites and the corresponding phase measurements Φ.

To linearize Eq. (2), we let $x_A = x_{A0} + \Delta x_A$, $y_A = y_{A0} + \Delta y_A$, $z_A = z_{A0} + \Delta z_A$, where $[x_{A0}, y_{A0}, z_{A0}]$ is a known reference position near the receiver, which can be estimated using code pseudoranging. Substituting the linearized version of Eq. (2) into Eq. (1) yields

$$\lambda\Phi_A^i(k) - \rho_{A0}^i(k) = a_x^i(k)\Delta x + a_y^i(k)\Delta y + a_z^i(k)\Delta z - \lambda n_A^i, \tag{3}$$

where

$$a_x^i(k) = -\frac{x^i(k) - x_{A0}}{\rho_{A0}^i(k)}, \quad a_y^i(k) = -\frac{y^i(k) - y_{A0}}{\rho_{A0}^i(k)}, \quad \text{and} \quad a_z^i(k) = -\frac{z^i(k) - z_{A0}}{\rho_{A0}^i(k)}. \tag{4}$$

Suppose the receiver is static and three satellites are continuously tracked from epoch 0 to epoch n, the linearized observation equations can be expressed in matrix form as

$$\mathbf{y} = \mathbf{A}\mathbf{x} + \mathbf{B}\mathbf{z} + \mathbf{v}, \tag{5}$$

where

$$\mathbf{y} = [\lambda\Phi_A^1(0) - \rho_{A0}^1(0), \lambda\Phi_A^2(0) - \rho_{A0}^2(0), \ldots]^T,$$

$\mathbf{x} = [\Delta x, \Delta y, \Delta z]^T$, $\mathbf{z} = [n_A^1, n_A^2, n_A^3]^T$, $\mathbf{v}$ is the measurement noise vector, and the matrices $\mathbf{A}$ and $\mathbf{B}$ are given by

$$\mathbf{A} = \begin{bmatrix} a_x^1(0) & a_y^1(0) & a_z^1(0) \\ a_x^2(0) & a_y^2(0) & a_z^2(0) \\ a_x^3(0) & a_y^3(0) & a_z^3(0) \\ a_x^1(1) & a_y^1(1) & a_z^1(1) \\ a_x^2(1) & a_y^2(1) & a_z^2(1) \\ a_x^3(1) & a_y^3(1) & a_z^3(1) \\ \vdots & \vdots & \vdots \end{bmatrix}_{3(n+1)\times 3}, \quad \text{and} \quad \mathbf{B} = \begin{bmatrix} -\lambda & 0 & 0 \\ 0 & -\lambda & 0 \\ 0 & 0 & -\lambda \\ -\lambda & 0 & 0 \\ 0 & -\lambda & 0 \\ 0 & 0 & -\lambda \\ \vdots & \vdots & \vdots \end{bmatrix}_{3(n+1)\times 3}. \tag{6}$$

3.1.3 Integer Least Squares

In the linearized observation equation Eq. (5), $\mathbf{x}$ and $\mathbf{z}$ are unknown real and integer vectors, respectively, which are to be estimated from the satellite data by using the maximum likelihood (ML) estimator:

$$(\mathbf{x}_{ML}, \mathbf{z}_{ML}) = \arg\max_{\mathbf{x},\mathbf{z}} P_{\mathbf{y}|\mathbf{x},\mathbf{z}}(\mathbf{y}|\mathbf{x}, \mathbf{z}), \tag{7}$$

where $(\mathbf{x}, \mathbf{z}) \in R^p \times Z^q$, and $P_{\mathbf{y}|\mathbf{x},\mathbf{z}}(\mathbf{y}|\mathbf{x}, \mathbf{z})$ is the probability of observing $\mathbf{y}$ given $\mathbf{x}$ and $\mathbf{z}$. Assuming the stochastic process $\mathbf{v}$ is Gaussian with zero mean and covariance $\mathbf{\Sigma}$, we have

$$(\mathbf{x}_{ML}, \mathbf{z}_{ML}) = \arg\min_{\mathbf{x},\mathbf{z}} (\mathbf{y} - \mathbf{A}\mathbf{x} - \mathbf{B}\mathbf{z})^T \mathbf{\Sigma}^{-1} (\mathbf{y} - \mathbf{A}\mathbf{x} - \mathbf{B}\mathbf{z}). \tag{8}$$

If we consider a block matrix $[\mathbf{A}\ \mathbf{B}]$ and the unknown vector $[\mathbf{x}\ \mathbf{z}]^T$, the floating solution $[\hat{\mathbf{x}}\ \hat{\mathbf{z}}]^T$ can be obtained by solving

$$[\mathbf{A}\ \mathbf{B}]^T \mathbf{\Sigma}^{-1} [\mathbf{A}\ \mathbf{B}][\hat{\mathbf{x}}\ \hat{\mathbf{z}}]^T = [\mathbf{A}\ \mathbf{B}]^T \mathbf{\Sigma}^{-1} \mathbf{y}, \tag{9}$$

Eliminating $\hat{\mathbf{x}}$ leads to the least-squares solution of $\hat{\mathbf{z}}$:

$$\hat{\mathbf{z}} = \mathbf{\Gamma}\mathbf{B}^T (\mathbf{I} - \mathbf{A}(\mathbf{A}^T \mathbf{\Sigma}^{-1} \mathbf{A})^{-1} \mathbf{A}^T) \mathbf{y}, \tag{10}$$

where $\mathbf{\Gamma} = (\mathbf{B}^T \mathbf{C}' \mathbf{B})^{-1}$ is the covariance matrix for $\hat{\mathbf{z}}$, and $\mathbf{C}' = \mathbf{\Sigma}^{-1} - \mathbf{\Sigma}^{-1}\mathbf{A}(\mathbf{A}^T \mathbf{\Sigma}^{-1} \mathbf{A})^{-1} \mathbf{A}^T \mathbf{\Sigma}^{-1}$.

In general, $\hat{\mathbf{z}}$ is a real vector and the ML solution can be found in the following least-squares sense [7, 12]:

$$\hat{\mathbf{z}}_{ML} = \arg\min_{\mathbf{z}} (\mathbf{z} - \hat{\mathbf{z}})^T \mathbf{\Gamma}^{-1} (\mathbf{z} - \hat{\mathbf{z}}) \ \text{ for } \ \mathbf{z} \in Z^q. \tag{11}$$

If $\mathbf{\Gamma}$ is diagonal, the solution for $\mathbf{z}$ can be found by rounding each component of $\hat{\mathbf{z}}$ to its nearest integer. This simple approach, however, does not work in realistic situations where the matrix $\mathbf{\Gamma}$ is typically not diagonal. As a result, simple rounding off will not give the correct estimate of $\mathbf{z}$ and the search for the true integer vector has to be performed over the entire integer space by using some efficient searching algorithm [5, 6, 11, 8, 16, 18]. Once $\hat{\mathbf{z}}_{ML}$ is found, the estimate of the real position vector $\mathbf{x}$ can be obtained by substituting $\hat{\mathbf{z}}_{ML}$ into the least-squares equation (8). This yields

$$\hat{\mathbf{x}}_{ML|\mathbf{z}} = (\mathbf{A}^T \mathbf{\Sigma}^{-1} \mathbf{A})^{-1} \mathbf{A}^T \mathbf{\Sigma}^{-1} (\mathbf{y} - \mathbf{B}\hat{\mathbf{z}}_{ML}). \tag{12}$$

It should be noted that the ambiguity fixing process (Eq. 11) breaks down Eq. (9), resulting in the above least squares ambiguity search (LSAS) algorithm not being an optimal one, i.e., it is not guaranteed that $(\hat{\mathbf{x}}_{ML|\mathbf{z}}, \hat{\mathbf{z}}_{ML}) = (\mathbf{x}_{ML}, \mathbf{z}_{ML})$. It has been shown that $(\hat{\mathbf{x}}_{ML|\mathbf{z}}, \hat{\mathbf{z}}_{ML})$ can be away from $(\mathbf{x}_{ML}, \mathbf{z}_{ML})$ and a more general searching criterion has to be used [19, 4, 26].

3.1.4 Scaling relation between convergence time and noise amplitude

In practice, we are most interested in cases when the positioning accuracy is high, or the probability of correct estimate of the integer ambiguity, P_c, is close to one. Particularly, we wish to know, given certain noisy environment, how long it will take us to achieve a desired value of P_c, where P_c is close to one. This can be addressed by investigating the influence of noise on P_c. In this study, P_c obtained from LSAS is used and $(\hat{\mathbf{x}}_{ML|\mathbf{z}}, \hat{\mathbf{z}}_{ML}) = (\mathbf{x}_{ML}, \mathbf{z}_{ML})$ is assumed for simplicity, since we are only concerned with large P_c and LSAS algorithm generally produces good results in this situation.

Assume $\mathbf{y}$ is a Gaussian variable, then $\hat{\mathbf{z}}$, a linear function of $\mathbf{y}$, is Gaussian too. We write $\hat{\mathbf{z}} = \mathbf{z} + \mathbf{u}$, where $\mathbf{u}$ is Gaussian with zero mean and covariance matrix $\mathbf{\Gamma}$. Multiplying both sides by $\mathbf{G} \equiv \mathbf{\Gamma}^{-1/2}$ and defining $\hat{\mathbf{y}} = \mathbf{G}\hat{\mathbf{z}}$, we get $\hat{\mathbf{y}} = \mathbf{G}\mathbf{z} + \hat{\mathbf{u}}$, where $\hat{\mathbf{u}}$ is a Gaussian random variable with zero mean and unit variance. Equation (11) can then be written in an equivalent form

$$\mathbf{z}_{ML} = \arg\min ||\hat{\mathbf{y}} - \mathbf{G}z||^2 \ \text{ for } \ \mathbf{z} \in Z^q. \tag{13}$$

The set $\{\mathbf{G}\mathbf{z} | \mathbf{z} \in Z^q\}$ constitutes a lattice in R^q. Equation (13) suggests that the maximum likelihood value of $\mathbf{z}$ can be found by computing the nearest lattice point to vector $\hat{\mathbf{y}}$. The probability P_c that $\mathbf{z}_{ML}$ is true is completely determined by the Venoroi cell. By definition of the lattice, a lower packing distance between two neighboring points can be computed by using

$$d \propto |\mathbf{G}|^{1/q}, \tag{14}$$

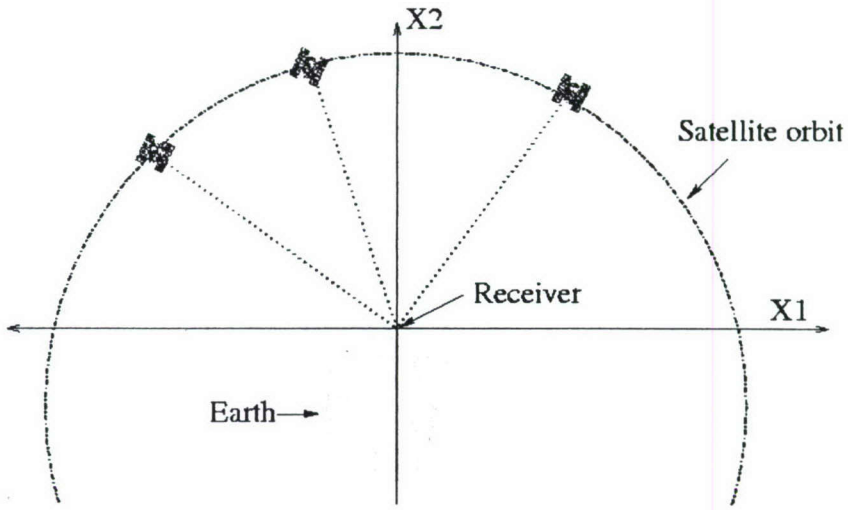

Figure 1: Synthetic 2-D GPS setup.

where $|\mathbf{G}|$ is the determinant of the matrix $\mathbf{G}$ and q, the number of unknown integers, is the dimension of $\mathbf{G}$. As a rough estimate, the distance d can be used to compute the lower bound of the probability P_c. Alternatively, given a desired value of P_c, there is a corresponding value of d that depends on factors such as the noise amplitude and the number of data samples. We emphasize, however, that such use of the rough estimate of the lower bound of P_c is only for the purpose of obtaining a scaling dependence of the convergence time on the noise strength, which by its nature is not precise. In fact, precise estimates of the lower and upper bounds have been obtained recently [18].

To be able to find a closed-form solution for $|\mathbf{G}|$, here we consider a two-dimensional (2D) GPS setup as shown in Fig. 1. All results based on this 2D model can be extended to the real three-dimensional GPS setup. Assume that there are q satellites tracked and the noise terms for the corresponding carrier-phase measurements are independent of each other with covariance matrix $\mathbf{\Sigma} = \sigma^2\mathbf{I}$. The inverse of $\mathbf{\Gamma}$ becomes

$$\mathbf{\Gamma}^{-1} = \frac{1}{\sigma^2}[\mathbf{B}^T\mathbf{B} - \mathbf{B}^T\mathbf{A}(\mathbf{A}^T\mathbf{A})^{-1}\mathbf{A}^T\mathbf{B}] = \frac{\lambda^2}{\sigma^2}\left[n\mathbf{I} - \frac{\mathbf{Q}}{d_1 d_3 - d_2^2}\right], \tag{15}$$

where

$$d_1 = \sum_{k=0}^{n}\sum_{i=1}^{q}[a_x^i(k)]^2, \quad d_2 = \sum_{k=0}^{n}\sum_{i=1}^{q}a_x^i(k)a_y^i(k), \quad \text{and} \quad d_3 = \sum_{k=0}^{n}\sum_{i=1}^{q}[a_y^i(k)]^2, \tag{16}$$

and $\mathbf{Q}$ is a $q \times q$ matrix with elements given by

$$Q_{ij} = d_3\sum_{k=0}^{n}a_x^j(k)\sum_{k=0}^{n}a_x^i(k) - 2d_2\sum_{k=0}^{n}a_x^j(k)\sum_{k=0}^{n}a_y^i(k) + d_1\sum_{k=0}^{n}a_y^j(k)\sum_{k=0}^{n}a_y^i(k). \tag{17}$$

Apparently, $|\mathbf{G}|^{1/q} = |\mathbf{\Gamma}^{-1}|^{1/2q}$ depends on both σ and n.

To find the relationship between σ and n for a given P_c, or equivalently, a constant $|\mathbf{\Gamma}^{-1}|$, we assume $[x_{A0}, y_{A0}] = [0, 0]$, the initial angle of satellite i is α, the orbital speed of the satellite is $\dot{\alpha}$, and the sampling period is T. We then have

$$\sum_{k=0}^{n}a_x^i(k) = -\sum\cos(\alpha + \dot{\alpha}kT) \approx -\sum\cos\alpha + \sin\alpha\sum\dot{\alpha}kT = \frac{1}{2}n^2T\dot{\alpha}\sin\alpha - (n+1)\cos\alpha, \tag{18}$$

where higher order terms of $\dot{\alpha}kT$ in the Taylor expansion are neglected. The approximation error is generally small since $\dot{\alpha}kT$ is relatively small. Similarly, we have

$$\sum_{k=0}^{n} a_y^i(k) \approx \frac{1}{2}n^2 T\dot{\alpha}\cos\alpha - (n+1)\sin\alpha \tag{19}$$

$$\sum_{k=0}^{n}[a_x^i(k)]^2 \approx \frac{1}{6}n(n+1)(2n+1)T^2\dot{\alpha}^2\sin^2\alpha - 2n^2T\dot{\alpha}\sin\alpha\cos\alpha + (n+1)\cos^2\alpha \tag{20}$$

$$\sum_{k=0}^{n}[a_y^i(k)]^2 \approx \frac{1}{6}n(n+1)(2n+1)T^2\dot{\alpha}^2\cos^2\alpha - 2n^2T\dot{\alpha}\sin\alpha\cos\alpha + (n+1)\sin^2\alpha \tag{21}$$

$$\sum_{k=0}^{n} a_x^i(k)a_y^i(k) \approx \frac{1}{6}n(n+1)(2n+1)T^2\dot{\alpha}^2\sin\alpha\cos\alpha - \frac{1}{2}n^2T\dot{\alpha} + (n+1)\sin\alpha\cos\alpha. \tag{22}$$

Substituting Eqs. (18) and (19) into Eq. (15), one can see that each entry in $\mathbf{\Gamma}^{-1}$ can be expressed as a second-order polynomial of n divided by σ^2. Thus, for increased σ, n has to be increased proportionally in order to maintain a desired positioning accuracy (or a constant $|\mathbf{\Gamma}^{-1}|$). This implies

$$n \propto \sigma, \tag{23}$$

for $n \gg 1$. While larger noise requires more data samples from the satellites, the linear relation indicates that, to achieve a desired positioning accuracy, the requirement is not as stringent as one would naively expect from $n \propto \sigma^2$. Our derivation suggests that if the satellites were kept static with respect to the static GPS receiver [i.e., $\dot{\alpha} = 0$ in Eq. (18)], then the scaling relation $n \propto \sigma^2$ would hold. It is the relative movement between GPS satellites and Earth surface that introduces another degree of dependence on n, resulting in a shorter estimation time than the static case. Note that the movement of the receiver will have similar effect if the velocity of the receiver is known exactly. This is in fact quite encouraging as it suggests that the integer parameter estimation time for kinematic GPS is likely to be shorter.

3.1.5 Simulation Results

Since the purpose of the simulations is to verify the theoretically derived dependence of the covergence time on the noise amplitude, it is necessary to be able to vary the noise variance in a systematic way. A synthetic 2D GPS setup, as illustrated in Fig. 1, is suitable for this purpose. The setup is similar to the one used in [16]. We assume that the position of the (GPS) receiver $\mathbf{x}$, which is to be determined, can be modeled as a zero-mean Gaussian random variable with certain variance in each dimension. The coordinate axes are chosen such that the origin is a point on the surface of the earth [a point on the periphery of a circle of radius equal to that of the earth $R_e = 6357$km]. We further suppose that there are three visible satellites orbiting the earth at the altitude of $20,200$km and with the period of 12 hours (angular velocity of $1/120s^{-1}$). The satellites transmit a carrier signal of wavelength $\lambda = 19$cm each, and their coordinates are known to the receiver. The receiver, which is assumed to be completely synchronized with the satellites (meaning that it can generate the transmitted carrier signals), measures the phases of the received carrier signals every $T = 2$s and unwraps them as times goes by. By multiplying these (unwrapped) phase measurements by the wavelength divided by 2π , the receiver can measure its distance (or range) to each satellite up to some additive noise, which is assumed to be $N(0.\sigma^2)$ and, of course, up to an integer multiple of the wavelength. (This integer multiple can be thought as the number of carrier signal cycles between the receiver and the satellite when the carrier signal is initially phase locked.) As we have described, by linearizing the range equations, the problem becomes one of estimating a real parameter $\mathbf{x}$ (the coordinates of the receiver) and an integer parameter $\mathbf{z}$ (the integer multiples of the wavelengths) in a linear model. In the simulation that follows, the actual location of the receiver is $\mathbf{x} = [50; 100]^T$, which will be estimated using the carrier-phase measurements. We assume that the standard deviation of $\mathbf{x}$ is 100m along each

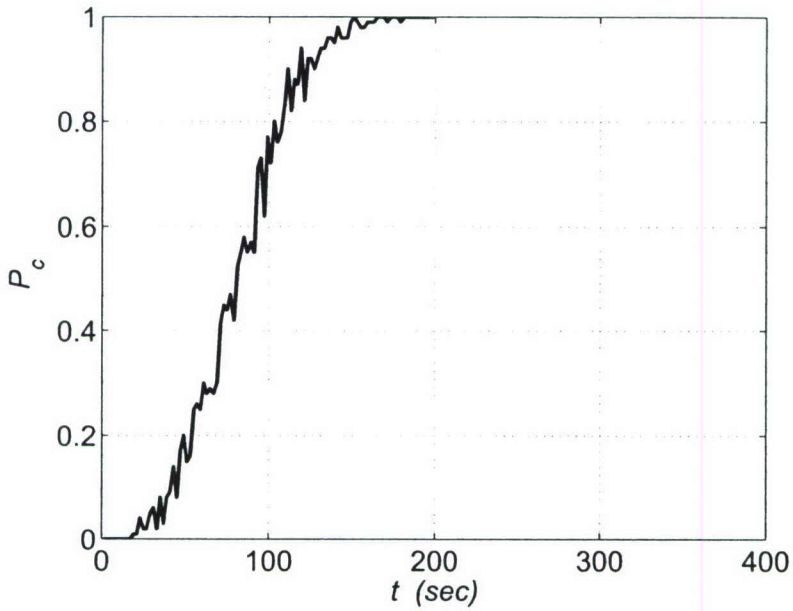

Figure 2: P_c versus time for $\sigma = 1$cm. Note that P_c after $t = 200s$ is almost equal to one in the simulation.

coordinate axis. The satellites make angles of 100, 130, and 50 degrees with the axis initially, and the direction of rotation for all of them is clockwise. The standard deviation of phase-measurement noise in units of length is assumed to be in the centimeter range. Using the carrier-phase measurements, the receiver tries to find its own position $\mathbf{x}$ (as well as the ambiguous integer multiples of the wavelengths) as a function of time by solving for the ML estimates.

Figures 2 and 3 show the results of the algorithm for $\sigma = 1$cm in terms of P_c and receiver positioning respectively. The exact value of the P_c is computed by Monte Carlo simulation of 1500 runs. It can be seen that the position estimation error reduces as the probability of correct integer estimation approaches unity. When the integer ambiguity is resolved correctly, the position estimation error is of the order of millimeters.

Having established the accuracy of the integer least-squares algorithm for static GPS positioning, we wish to evaluate its performance in the presence of noise. For this purpose, the algorithm was provided with various values of phase measurement noise variance as input. The range of σ varied from 0.2cm to 2cm with increment of 0.2cm. The values of P_c for all cases were calculated using 1500 Monte Carlo simulations. Figure 4 shows P_c versus time for various σ values. It is observed that as σ increases, the time it takes to achieve a certain level of P_c also increases. The family of curves in Fig. 4 can be used to calculate the maximum allowable noise variance for a given amount of observation time and required value of P_c. For example in Fig. 4, if the observation time is 150 s and the integer ambiguity estimate is to be reliable with 90% accuracy ($P_c = 0.9$), the maximum allowable noise variance is about 1.2cm.

Figure 5 shows the linear relation characterizing the sensitivity of performance to noise amplitude, as predicted by our theoretical analysis. A use of this result is that the performance of integer least-squares algorithm can be predicted for a given noise level.

3.1.6 Discussions

We have addressed the performance of integer least-squares algorithm for GPS signals in noisy environments. Mathematically, integer ambiguity resolution is equivalent to searching for the integer vector closest to a given

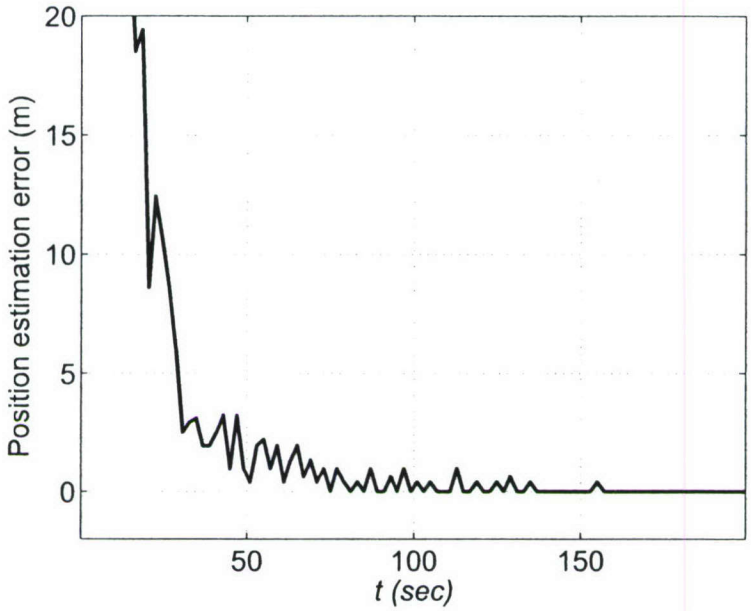

Figure 3: Position estimation error (meters) versus time (sec), where the initial errors ($t < 20s$) are large and not shown in the figure.

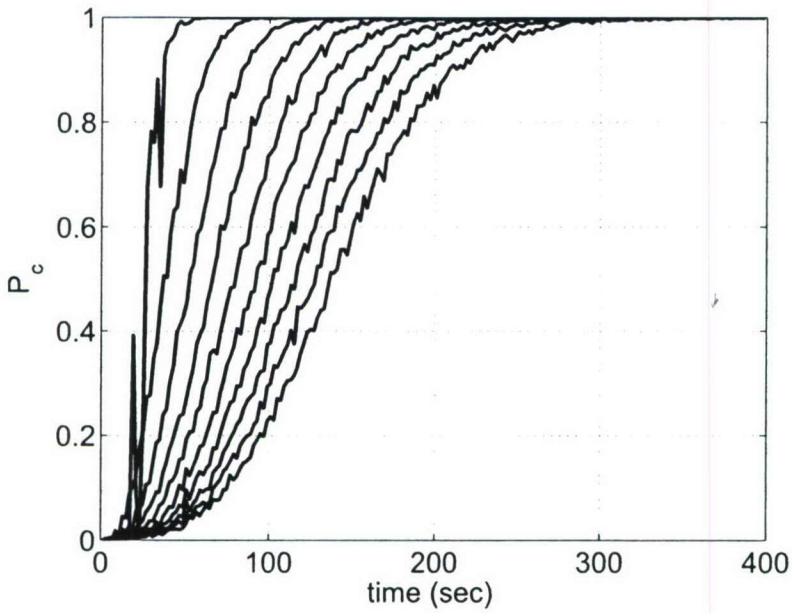

Figure 4: P_c versus time for σ values ranging from 0.2cm to 2cm (from left to right). Maximum allowable noise variance for given values of time and P_c can be determined accordingly.

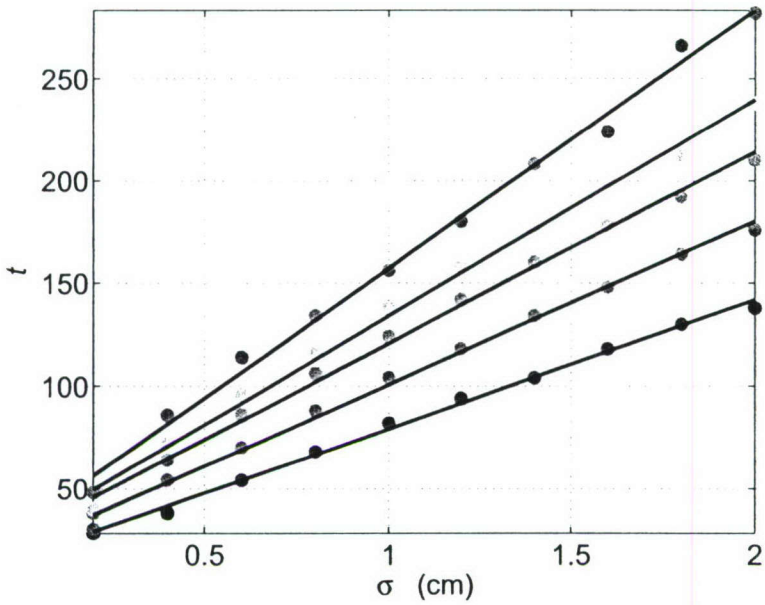

Figure 5: Sensitivity of performance to measurement noise variance. From top to bottom: $P_c = 0.99, 0.95, 0.9, 0.75, 0.5$ respectively.

real vector on an integer lattice. In a noisy environment, the probability of error can be significantly large. We find that the observation time required to achieve a fixed value of a lower bound of P_c and thus P_c itself is directly proportional to the standard deviation of phase-measurement noise, in contrast to the naive expectation that the time is proportional to the variance of the phase noise. This suggests the possibility of achieving short convergence time even if large noise is present.

It should be noted that we have assumed an ideal system model in this study. For example, systematic errors are assumed to be eliminated by using double differencing, and the resulted system errors are approximately Gaussian with zero mean. This may not be true in practice, especially when long baselines are utilized. In this situation, additional modeling of large residual errors has to be employed, e.g., the means of residual ionospheric and tropospheric errors have to be estimated together with $\mathbf{x}$ and $\mathbf{z}$. If the means of these residual errors remain constant or change slowly during the process of ambiguity resolution, the convergence time of ambiguity resolution will only be delayed approximately by a constant, the overall linear relationship between the time and the noise amplitude should still hold.

We also remark that the main objective of our work is to obtain a *scaling* relation between the convergence time and the noise strength, which is an order-or-magnitude type of estimate. The reason is that the convergence time depends on too many algorithmic and system details and it is not possible to give precise numbers to characterize it. For this purpose we have based our theoretical analysis on the upper and lower bounds in the probability of correct resolution of the integer ambiguity given in [16], as the required computational time is only polynomial. However, these bounds can be poor and much tighter bounds can be found in Ref. [18]. We wish to emphasize that the results obtained for the performance in the presence of noise are based on the integer least-squares principle in general and thus they should not be dependent on the specific search method used.

For future directions, parallel algorithms taking advantage of multiple satellite signals to reduce the ambiguity-resolution time should be pursued. In addition, the study for the effect of noise on GPS positioning should be extended to kinematic GPS positioning algorithms. It is also recommended to develop a particle-filter based algorithm and to compare its sensitivity to noise with those of integer least-squares algorithms for both static and

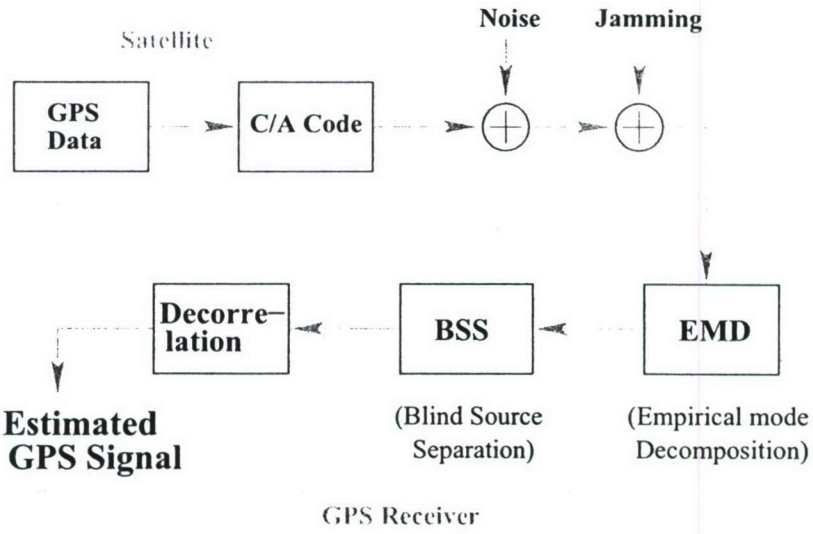

Figure 6: Block diagram of our proposed GPS antijamming scheme.

kinematic positioning.

3.2 Empirical Mode Decomposition and Application to Anti-jamming for GPS Signals

3.2.1 Background

GPS signals are direct-sequence (DS) spread-spectrum signals and therefore have some degree of inherent noise immunity [27]. After despreading the received signal, the original satellite signal can be collapsed into a narrow bandwidth about the carrier frequency, while the jamming signals are spread due to the lack of correlation with the pseudo-random code that encodes the satellite information. A portion of the spread jamming signal remains within the frequency band entering the tracking loop with the satellite signal. Thus signal tracking can be stable only if the jamming-to-signal ratio (JSR) is below the processing gain of the spreading code. In general, a JSR of greater than 40dB is likely to prevent the GPS receiver from tracking the satellite signal and from estimating its own position.

There are situations where jammers may be much stronger than the GPS signals, and are located at close physical proximity to the GPS receiver. In such a case, the spreading gain of the spread-spectrum system might not be sufficient to decode the satellite data reliably. In fact, one of the major difficulties in time-space position information (TSPI) design in defense applications is jamming rejection. During the project period, we developed a procedure based on the empirical-mode decomposition (EMD) method [28], in combination with the traditional blind source separation (BSS) technique, as a receiver-based algorithm to suppress jamming. For practical implementations, our algorithm may be integrated into the software radio such as the one described in Ref. [29]. Schemes similar to ours have been suggested for applications in different contexts, such as biomedical signal processing, notably in Refs. [30] and [31] where a combination of EMD and independent component analysis was employed.

The traditional Fourier analysis is powerful for stationary (or piecewise stationary) signals. While the wavelet method can handle nonstationary signals, it is essentially an *adjustable* window Fourier spectral analysis and therefore fundamentally it is also a linear method. The method of EMD was pioneered by Huang et al. to specifically deal with nonstationary and/or nonlinear signals [28]. That jamming signals in GPS applications are likely to be nonstationary and possibly nonlinear motivates us to investigate the applicability of EMD-based methods for antijamming. The block diagram of our proposed method is shown in Fig. 6, where the original

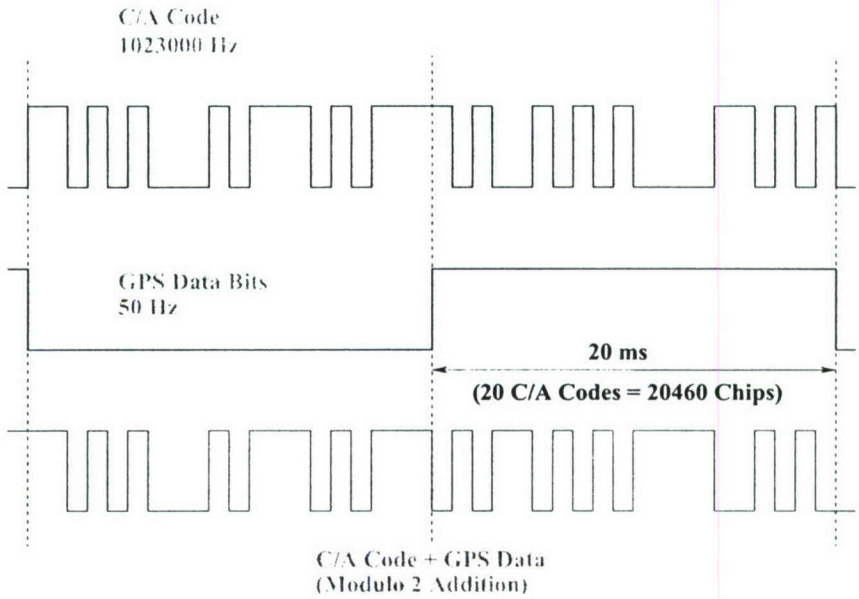

Figure 7: GPS direct-sequence spread-spectrum signal structure (C/A code).

GPS data that carry the satellite information are encoded and both noise and jamming are present in the received GPS signal. The EMD/BSS combined procedure decomposes the jammed GPS signal into a number of modes of distinct time scales. Since the code that encodes the satellite information (the C/A code) is also known at the receiver end, a decorrelation procedure can be used to identify the modes that contain mostly the original GPS data. We shall detail our method and provide strong evidence that the method works for nonstationary jamming of JSR of up to 45 dB.

In the following we provide a brief background of the GPS signal structure and discuss several existing antijamming methods. We then describe the EMD and BSS methods and their implementations and present simulation results with GPS signals.

3.2.2 GPS signal structure and existing antijamming methods

GPS consists of 24 satellites orbiting at the altitude of 20,183 km, of known positions. The signals transmitted by the GPS satellites are direct-sequence spread-spectrum (DSSS) signals that consist of three portions: the Course Acquisition (C/A) code on the L1 carrier (1.575GHz), the P-code on the L1 carrier, and the P-code on the L2 carrier (1.227GHz). The C/A code has a chip-rate of 1.023MHz and a period of 1msec, while the P-code, for military use only, has a chip-rate of 10.23MHz and a period of 1 week. As shown in Fig 7, with Binary Phase Shift Keying (BPSK) modulation, the resulting C/A-code signal requires a bandwidth of 2×1.023MHz for transmission, and the P-code signal needs a bandwidth of 2×10.23MHz.

A GPS receiver receives DSSS signals from four or more satellites and estimates the code-phase differences and/or carrier-phase differences in order to calculate its own position [2]. As shown in Fig. 8, the GPS receiver contains two tracking loops: code-phase tracking loop and carrier-phase tracking loop. Code tracking and de-spreading are performed prior to carrier tracking since the power of the received GPS signal is much lower than the background noise and sufficient signal-to-noise ratio (SNR) necessary for carrier-phase tracking can only be achieved by code despreading. The pseudo-random noise (PN) generator generates a PN sequence identical to the C/A or the P code to synchronize with the input signal from a GPS satellite. The code correlator sweeps the uncertainty ranges of the input-code phase at discrete steps, and detects the coarse synchronization (acquisition) of the code phases between the input and local signals by finding the maximum of the correlation function. The

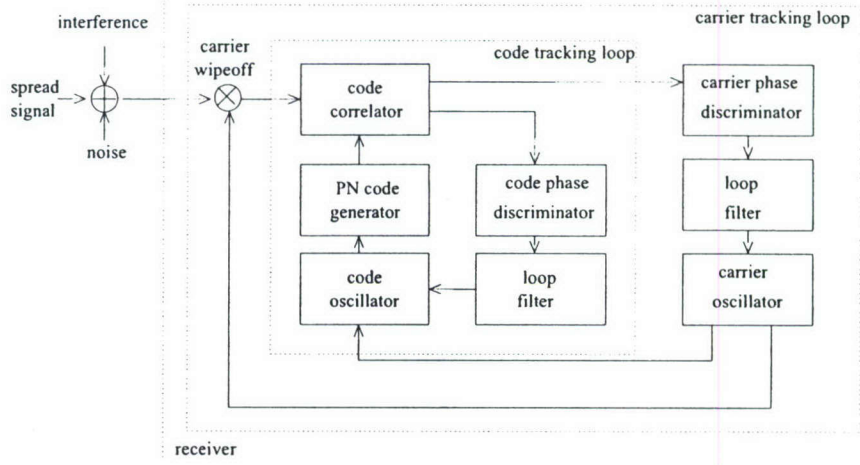

Figure 8: Block diagram of a GPS receiver that typically consists of a code and a carrier-phase tracking loop.

code-phase tracking loop can track the variations of the incoming code phase and keeps the code-phase alignment error within an allowable limit after the code-phase acquisition. From accurate tracking of the code phase, the pseudo-range time delay can be obtained and the input signal is despread to yield encoded navigation and timing information. The despread signal is then passed on to the carrier-phase tracking loop for ranging.

In a hostile environment where jamming sites may be close to GPS users, a huge JSR is possible. Thus, in order for GPS receiver to function, jammer should be either rejected before the tracking loops or reduced/eliminated inside the tracking loops. For the first case, the structure of conventional tracking loops does not require change, while for the second case, novel algorithms need to be designed.

There are a number of ways to mitigate the effects of jamming on GPS receivers before the signal enters the tracking loops. These are (1) time-domain filtering [32, 33], (2) frequency-domain filtering [34, 35], (3) spatial filtering [24, 36], and (4) time-frequency filtering [22, 37]. The first two types of filtering are conventional. The third type typically uses adaptive nulling antenna, an array of antenna elements. Spatial filters have the ability to modify its reception pattern, i.e., different amplification rates for signals from different directions of arrival (DOA). Based on the assumption that jamming signals and satellite signals have different DOA, adaptive nulling antenna can emphasize the desired GPS satellite signals and reject the jamming signals [24]. The technique is effective for both narrow- and broad-band jamming signals. However, due to multi-path propagation of signals and constraints on its size and power, adaptive antenna alone cannot provide an acceptable interference mitigation. The fourth type (time-frequency filtering) relies on the assumption that broad-band satellite and jamming signals have distinct time-frequency signatures. Once the instantaneous frequencies of the jamming signals are estimated from the received signals, techniques such as time-varying notch filter [22] or subspace projection [37] can be used to reduce or eliminate the jamming. A possible drawback is that time-frequency filters tend to block the frequencies occupied by jamming signals, and thus also subtract the power of satellite signals at those frequencies from the total power of the received signals. If jamming signals occupy a substantial bandwidth in the signal spectrum, the filtered signals will be significantly distorted. Thus, in general, this method is more effective for narrow-band jamming signals.

The conventional code-tracking loop utilizes delay-lock loop (DLL), which offers little protection against jamming and multipath. One way to increase the robustness of DLL is to include models (e.g., AR model) for jammer signals and multipath in the DLL. The resulting DLL can then estimate the code delay using adaptive algorithms, e.g., Kalman filters and/or particle filters [38, 39].

Our proposed EMD/BSS procedure is fundamentally a nonlinear signal-processing method and it is therefore different from these existing linear methods.

3.2.3 Nonlinear antijamming: proposed EMD/BSS methodology

Our method applies EMD to the received jammed GPS signal to decompose it into a number of intrinsic mode functions (IMFs), which can be regarded as multiple observations of a random process. Assuming that these observations are linear combinations of the original signal, a BSS technique can be used to extract the GPS signal from the IMFs.

EMD method. Traditional methods such as the Fourier spectral analysis assume stationarity and/or approximate the physical phenomena with linear models. These approximations may lead to spurious components in the time-frequency distribution diagrams if the underlying signal is nonstationary and nonlinear. Empirical Mode Decomposition (EMD) is a technique [28] to deal specifically with nonstationary and nonlinear signals. Given such a signal, the method adaptively decomposes it into a number of modes (IMFs) that are topologically equivalent to amplitude- and frequency-modulated, sinusoidal signals. In the analytic-signal representation, the modes correspond to proper rotations [28]. Thus the EMD method naturally yields estimates of the significant instantaneous frequencies embedded in the signal, by performing the Hilbert transform on each IMF. The ease and accuracy with which the EMD method processes nonstationary and nonlinear signals have led to its widespread use in various applications such as seismic data analysis [28], chaotic time series analysis [40, 41], and meteorological data analysis [42], etc.

Given a signal $X(t)$, the EMD method focuses on the level of local oscillations and decomposes the signal into a finite and often a small number of fundamental oscillatory modes. The bases (IMFs) into which the signal is decomposed are obtained from the signal itself, and they are defined in the time domain. They are of the same length as the original signal and preserve the frequency variations with time. The base modes can be made approximately complete and nearly orthogonal with respect to each other. Here, completeness implies that the original signal can be reconstructed without any loss of information by simply summing up the IMFs. Thus, the IMFs can be viewed as linear components of the original or source signal $X(t)$. In order to achieve this, two conditions need to be satisfied: (1) the total number of extrema of IMF(t) be equal to the number of zero crossings, and (2) the mean of the upper envelope IMF$_u(t)$ and the lower envelope IMF$_l(t)$ be zero. The process to obtain the IMFs from the signal is called *sifting*, which consists of the following steps: (1) identification of the extrema of $X(t)$, (2) interpolation of the set of maximal and minimal points (say, by using cubic splines) to yield an upper envelope $X_u(t)$ and a lower envelope $X_l(t)$, respectively, and their average $m(t) \equiv [X_u(t) + X_l(t)]/2$, (3) subtraction of the average from the original to yield $d(t) = X(t) - m(t)$, and (4) repetition of steps (1-3) until $d(t)$ satisfies the two conditions for being an IMF. Once an IMF is generated, the residual signal $r(t) = X(t) - \text{IMF}_1(t)$ is regarded as the original signal, and steps (1-4) are repeated to yield the second IMF, and so on. The procedure is complete when either the residual function becomes monotonic, or when the amplitude of the residue falls below a pre-determined small value so that further sifting would not yield any useful components. These features guarantee the computation of a finite number of IMFs within a finite number of iterations. The outcome of the EMD procedure is the following decomposition of the original signal:

$$X(t) = \sum_{i=1}^{n} \text{IMF}_i(t) + r(t) \tag{24}$$

where IMF$_i(t)$ is the ith IMF, n is the total number of IMFs, and $r(t)$ is the final residue that has near zero amplitude and frequency.

Figure 9 shows the IMFs obtained from a simulated GPS signal to which a zero-mean and unit-variance Gaussian noise and a stationary, sinusoidal jamming signal are added. The GPS signal has the amplitude of 2 and the jamming amplitude is 200 (corresponding to JSR of 40dB). The top left panel shows the noisy and jammed GPS signal, and the seven remaining panels show the seven significant IMFs. We note that the first IMF in the top right panel visually resembles the original GPS signal. This example thus illustrates that for stationary jamming, the EMD method is capable of directly separating the GPS signal from the jamming. However, this appears not to be the case for nonstationary jamming, as shown in Fig. 10, where the top left panel is the noisy and jammed GPS signal. The jamming is a frequency-modulated signal with normalized frequency increased linearly from 0

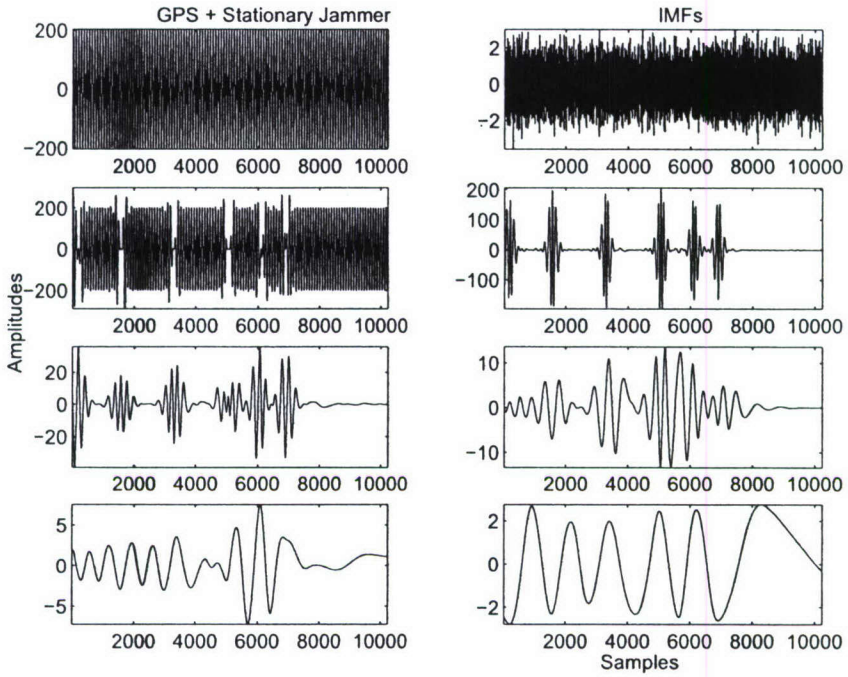

Figure 9: IMFs of a noisy and jammed GPS signal, where the jamming is stationary and the noise is Gaussian. The first IMF (upper right panel) is approximately the original GPS signal.

to 0.5 in the time interval considered. We find that none of the seven IMFs shown (in the remaining 7 panels) looks like the original GPS signal, which is in fact embedded in all IMFs. It is thus necessary to invoke a proper BSS procedure to extract the GPS signal.

Blind Source Separation. Blind Source Separation (see [43] for a review) is a method to extract basic source signals from several observed mixtures. It is considered "blind" because the source signals are not observed and no information is available about the observed mixtures. An *a priori* assumption is that the sources are independent of each other and they are not all white noise. BSS is particularly suitable for situations where different observations of the same sources are received from different sensors. The BSS technique has found applications in areas such as communications and biomedical signal processing [44, 45, 46].

Consider the time varying vector of observations

$$\mathbf{X}(t) = [X_1(t), .., X_k(t)]^T \tag{25}$$

obtained as a mixture from k sources

$$\mathbf{S}(t) = [S_1(t), .., S_k(t)]^T \text{ and} \mathbf{X}(t) = \mathbf{A}\mathbf{S}(t) \tag{26}$$

where $\mathbf{A}$ is the mixing matrix. We reconstruct the sources

$$\mathbf{Y}(t) = \mathbf{B}\mathbf{X}(t) \tag{27}$$

where $\mathbf{B}$ is a matrix to be determined, by adopting the criterion of minimizing mutual information. This requires the estimation of joint entropy, which is computationally expensive, and therefore we adopt the idea of Gaussian Mutual information [47] that requires computation only up to second-order characteristics.

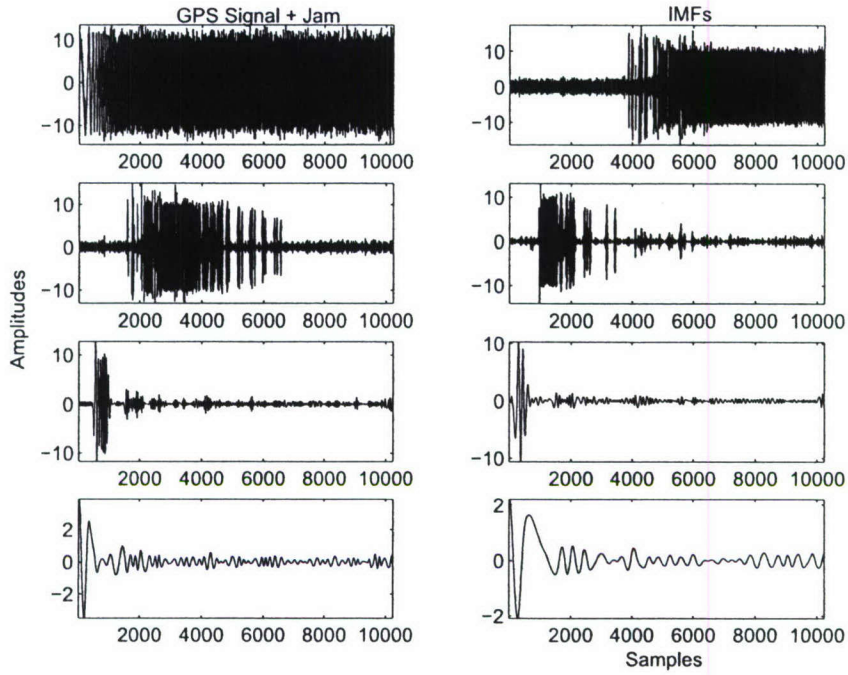

Figure 10: IMFs of a noisy and jammed GPS signal, where the jamming is nonstationary and the noise is Gaussian. In this case, the original GPS signal is spread over all IMFs.

3.2.4 Simulation Results

For simulation purposes, we have used the following baseband model for received GPS signals:

$$r(t) = c(t)d(t) + j(t) + n(t), \tag{28}$$

where $r(t)$ is the received signal, $c(t)$ is the spreading sequence, $d(t)$ is the transmitted GPS information symbol, $n(t)$ is the noise, and $j(t)$ is the jamming. In the simulation, the length of spread sequence is varied from 10 to 20 bits. For stationary jamming simulations, pure sinusoids of frequency 0.2 to 0.5 times the sampling frequency are chosen. Nonstationary jamming is modeled as a chirp signal with frequency changing from 0 to 0.5 times the sampling frequency. The amplitude of the transmitted GPS signal is normalized to unity, while the jamming amplitude is varied so that the maximal JSR is 45dB.

The code for EMD is adapted from the one developed by Rilling et al. [Matlab codes (G. Rilling, P. Flandrin and P. Goncalves), http://perso.ens-lyon.fr/patrick.flandrin/emd.html]. During a run, typically between 8 and 10 IMFs are generated. As can be seen from the time-series plots in Fig. 9, from the IMFs of stationary jammed GPS signal we can visually distinguish the jammer from the GPS signal. The GPS signal is captured almost entirely in the first mode, whereas the jammer is captured in the 2nd and 3rd modes. In this case, the BSS procedure is not necessary. To recover the GPS signal, it is a relatively simple matter of correlating the mode that contains the GPS signal with the PRN code. For nonstationary jammer, as in Fig. 10, both the GPS and the jamming are mixed in all the IMFs. In this case, it is necessary to use the BSS to extract the GPS signal. In particular, the IMFs can be regarded as multiple observations of the received signal. We adapted the code from the BLISS project [BSS Demonstration Code (http://www-lmc.imag.fr/SMS/SASI/bliss.html)] for BSS.

Figure 11 shows the result of extracting the GPS signal in the presence of stationary jamming, where the two top panels show the original GPS and the original jamming signals, respectively, and the two lower panels show the extracted GPS and jamming signals. A typical result with nonstationary jamming is shown in Fig. 12. It is

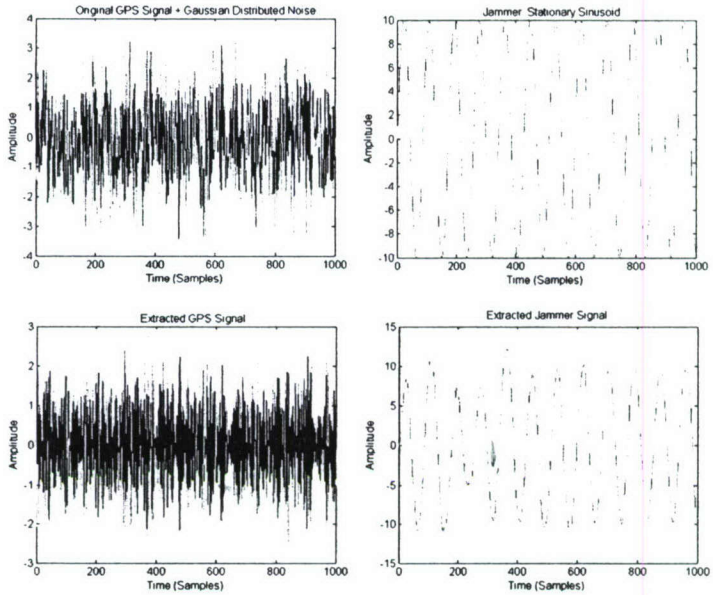

Figure 11: Result with stationary jammer. Upper panels: original GPS signal and jammer. Lower panels: extracted GPS signal and jammer.

apparent that our combined EMD/BSS methodology is capable of estimating the GPS signal in the presence of strong jamming, stationary or nonstationary.

To quantify the "goodness" of our method, we examine the bit error rate. In particular, information bits associated with the extracted GPS signal are compared with those in the original GPS signal. A typical result for one C/A code is shown in Fig. 13, where the ratio of bits received correctly to the number of bits transmitted versus the jamming signal amplitude is plotted. The upper and lower traces show the ratio for stationary and nonstationary jamming, respectively. We see that for stationary jamming, the information bit can be extracted with certainty. For nonstationary jamming of JSR of as high as 45dB, the percentage of correctly extracted bit is above 80%. Since one GPS bit (**0** or **1**) is modulated using 20 C/A codes, setting a conservative threshold, say at unity, for the ratio between the number of correctly estimated bits and that of the wrong bit can guarantee the extraction of the correct bit. For example, suppose the original bit is **1** and the JSR is 40dB, then out of the 20 C/A codes, **1** will appear approximately 16 times and **0** (the wrong bit) will appear about 4 times. The ratio is then 4, which can be distinguished from 1 almost certainly. Figure 13 suggests that our EMD/BSS method can perform to extract GPS satellite information in the presence of nonstationary jamming of JSR up to about 45dB.

3.2.5 Discussions

Intentional jamming of GPS signals is a serious concern especially for military applications. The nature of the GPS signal, i.e., its extreme low signal intensity, makes it vulnerable to jamming. In applications where dependence on GPS is high, a jammed GPS signal could have disastrous consequences. Thus it is of tremendous interest and importance to explore practical antijamming schemes.

We proposed and tested a simple yet effective antijamming algorithm which can be implemented in the receiver stage after the acquisition of the GPS signal. The algorithm makes use of two available techniques for data analysis: the Empirical Mode Decomposition method and the Blind Source Separation method based on Gaussian Mutual Information. We showed that the algorithm is capable of accurate estimation of GPS signal bits in the presence of stationary or nonstationary jammers. In particular, simulation results indicate that the GPS

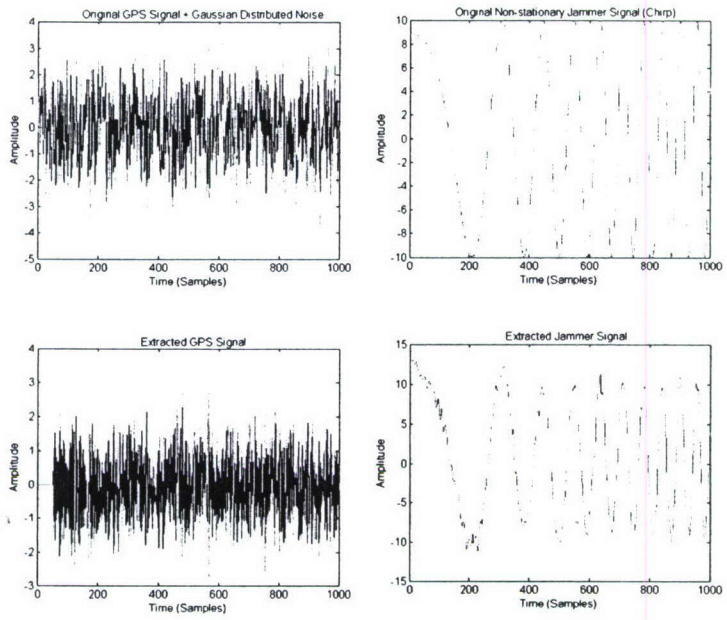

Figure 12: Result with nonstationary jammer. Upper panels: original GPS signal and jammer. Lower panels: extracted GPS signal and jammer.

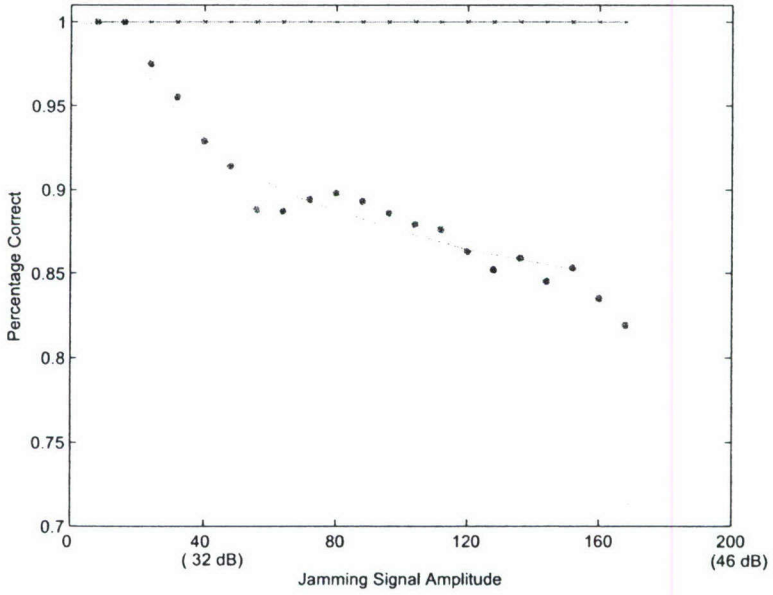

Figure 13: For one C/A code, the percentage of correctly extracted number of GPS signal bits versus the jamming amplitude. The upper trace is for stationary jammer and the lower for nonstationary jammer. Since one GPS information bit is encoded using 20 C/A codes, for JSR of up to 45dB, the correct bit can be obtained with certainty.

data can be decoded accurately with no error for nonstationary jammer of JSR of up to about 45dB.

For nonstationary jammer of JSR above 50dB, the performance of our method deteriorates. The solution may be to combine this algorithm with spatial filtering methods such as those described in [24, 36]. Another possibility is to integrate Kalman or particle filtering in the algorithm for estimating the phase/code delay. The model for such a system would assume the presence of jamming interference and, when combined with our algorithm, might enable GPS signal processing in the presence of exceedingly strong jammer.

3.3 Precise GPS positioning of moving objects in noisy environment by particle filters

3.3.1 Background

The problem of estimating the time-varying state of a system based on experimental measurements or observations finds many applications in physics, biology, and engineering. Examples include quantum state reconstruction and purity estimation [48, 49], noise reduction and state reconstruction in chaotic dynamical systems [50, 51], estimation of bounds on isocurvature perturbations in the Universe and on cosmic strings from cosmic microwave background and large-scale structure data [52, 53], gravitational wave signal analysis [54, 55], macromolecular structure determination [56, 57], prediction of protein-protein interactions from genomic data [58], tracking and positioning problems [59], etc. In general, a system model that evolves the state vector (x) in time is needed, so is an observational model that relates an observation vector (y) to the state vector. In any realistic application both noise and model uncertainties exist, rendering necessary a probabilistic treatment of the estimation problem. That is, one can evolve x according to the system model, and make corrections to or update x based on the available y. The quantity of interest is the posterior probability density function (pdf) $p(x|y)$, given all available observations y. The standard approach to addressing this problem is Bayesian inference [60], which leads to the classical Kalman filter when both the system and the observational models are linear. For nonlinear problems, a viable approach is *sequential Monte-Carlo simulation* (or particle filter) [61, 62, 63], which uses a set of random samples to approximate the posterior pdf $p(x|y)$. The approximated pdf evolves and is corrected by the observation based on the Bayes rule. If the number of samples is sufficiently large, the approximation approaches the optimal Bayesian estimate. Due to the constant improvement of modern computing technology, the sequential Monte-Carlo approach has begun to find significant applications in science and engineering [62, 63, 64].

A fundamental question in sequential Monte-Carlo simulations is how the precision of the estimated state vector depends on noise in the system and in the observation. Another issue of significant practical interest is how to deal with occasional but large disturbances, or *outliers*, in the observation. During the project period, we addressed these two related problems. In particular, we derived and verified a self-consistent equation that relates the covariance matrix of the samples, which determines the precision of the state estimate, to the covariance matrices of the system noise and of the observational noise. In addition, we proposed a robust sequential Monte-Carlo scheme to overcome the effect of outliers. In this regard, previous approach includes using heavy-tailed error distribution to improve the state-space models so that they react quite flexibly to changes in points or edges, but still provide smooth fits in other regions [65]. Leave-k-out diagnostic is used to detect a series of consecutive outliers for a linear state space model [66]. It uses all residual observations in the time span to check whether a series of consecutive observations are jointly outlying, thus it is actually "off-line". Our idea is to detect the outliers from the previous knowledge about the system and then to eliminate them in the sequential Monte-Carlo implementation. Simulations using a precise GPS positioning problem demonstrate the power of our scheme. We expect our results to have significant impacts on problems where the underlying system and/or experimental observations are subject to outliers. For example, the observation of a star or a galaxy may be corrupted by the drastic activity of another celestial body in a short period. In biological physics, macromolecular structure is inferred indirectly from various measurements, e.g. nuclear magnetic resonance spectra, X-ray reflections, or homology-derived restraints, which can easily contain outliers [56]. In GPS (global positioning system)-based precise positioning problems, GPS signals may be disturbed by sudden and large jamming.

In the following, we outline the basic steps of sequential Monte-Carlo method and derive a self-consistent equation governing the dependence of estimation error on noise. We then present a robust sequential Monte-Carlo scheme for mitigating the effect of measurement or observational outliers and provide numerical support.

3.3.2 Sequential Monte-Carlo method

Let $y(0:t) = \{y(t'), t' = t_0(=0),\ t_1,\ t_2,\ \cdots, t_k(=t)\}$ be the observations from time 0 to time t, which are not necessarily equidistant in time. We seek to obtain the posterior pdf $p[x(t)|y(0:t)]$. The state and observational equations are

$$x(t) = f[x(t_{k-1}), v(t_{k-1})], \tag{29}$$

$$y(t) = g[x(t), e(t)], \tag{30}$$

which describes the evolution of the state and maps the state to the observational vector, respectively, f and g can be nonlinear functions. The processes $v(t)$ and $e(t)$ represent random fluctuations (e.g., noise, uncertainties, outliers, etc.) in the system and in the observation, respectively. Often, in an application the distribution of the initial state can be obtained by considering the specific physics involved. It is thus reasonable to assume that this distribution is available. The pdf $p[x(t)|y(0:t)]$ can then be obtained recursively by prediction through the dynamical equation (29) and likelihood correction through the observational equation (30). In particular, given the pdf $p[x(t_{k-1})|y(0:t_{k-1})]$ at time t_{k-1}, the prediction step uses the dynamic equation (29) to obtain the prior pdf of the state at time t via the Chapman-Kolmogorov equation

$$p[x(t)|y(0:t_{k-1})] = \int dx(t_{k-1}) \cdot p[x(t)|x(t_{k-1})] \cdot p[x(t_{k-1})|y(0:t_{k-1})], \tag{31}$$

where $p[x(t)|x(t_{k-1}), y(0:t_{k-1})] = p[x(t)|x(t_{k-1})]$ is used. At time t, a new measurement $y(t)$ becomes available, which can be used to correct the prior pdf via the Bayes rule

$$p[x(t)|y(0:t)] = \frac{p[y(t)|x(t)]p[x(t)|y(0:t_{k-1})]}{p[y(t)|y(0:t_{k-1})]}, \tag{32}$$

where

$$p[y(t)|y(0:t_{k-1})] = \int p[y(t)|x(t)] \cdot p[x(t)|y(0:t_{k-1})]dx$$

depends on the likelihood function $p[y(t)|x(t)]$. The recurrence relations (31) and (32) form the basis for optimal Bayesian solution. For Gaussian noise, when f and g are linear functions, the recurrence relation can be solved analytically, which is the classical Kalman filter. For nonlinear functions f and g, a linearization technique is viable which leads to the so called extended Kalman filter [67]. Unscented Kalman filter deliberately selects a set of points and propagate them through the nonlinearity to estimate the Gaussian approximation [68]. While for more general cases, the approach of sequential Monte-Carlo simulation is desirable [61, 62, 63, 64].

Let $\{x_i(t),\ w_i(t)\}_{i=1}^N$ denote a random measure that characterizes the posterior pdf $p[x(t)|y(0:t)]$, where $\{x_i(t),\ i = 1,\ \ldots, N\}$ is a set of support points with associated weights $\{w_i(t),\ i = 1,\ \ldots, N\}$. The weights are normalized that $\sum_i w_i(t) = 1$. The posterior pdf can be approximated as

$$p[x(t)|y(0:t)] \simeq \sum_{i=1}^{N} w_i(t)\delta(x(t) - x_i(t)),$$

where $\delta(x)$ is the Dirac delta function such that $\delta(x) = 0$ if $x \neq 0$ and $\int_{x_1}^{x_2} \delta(x)dx = 1$ if $(x_1,\ x_2)$ contains 0. The average of an arbitrary function $f(x)$ can be simplified as

$$\langle f[x(t)]\rangle = \int f(x)p[x|y(0:t)]dx = \sum_i w_i(t)f[x_i(t)].$$

The weights are chosen using the principle of importance sampling [69]. In particular, given an arbitrary pdf $p(x)$, it may be difficult to draw samples. Suppose for an alternative pdf $q(x)$, samples can be drawn relatively easily. Letting $x_i \sim q(x)$ $(i = 1, ..., N)$ be samples drawn from some $q(\cdot)$, the *importance density*, we obtain the following weighted approximation:

$$p(x) \simeq \sum_{i=1}^{N} w_i \delta(x - x_i),$$

where $w_i \propto p(x_i)/q(x_i)$ is the normalized weight of the i'th sample.

Now consider the joint probability $p[x(0:t)|y(0:t)]$. In case of independent noise samples, we can write

$$p[x(0:t)|y(0:t)] \propto p[x(0)|y(0)] \prod_{j=1}^{k} p[y(t_j)|x(t_j)] p[x(t_j)|x(t_{j-1})].$$

Thus

$$\begin{aligned} p[x(0:t)|y(0:t)] &= p[x(t), x(0:t_{k-1})|y(t), y(0:t_{k-1})] \\ &= \frac{p[y(t)|x(t)]p[x(t)|x(t_{k-1})]}{p[y(t)|y(0:t_{k-1})]} p[x(0:t_{k-1})|y(0:t_{k-1})], \end{aligned}$$

Assume the posterior distribution $p[x(0:t_{k-1})|y(0:t_{k-1})]$ is approximated by $\{x_i(0:t_{k-1}),\ w_i(t_{k-1})\}_{i=1}^{N}$, given a new observation $y(t)$, the objective is to obtain an approximation $\{x_i(0:t),\ w_i(t)\}_{i=1}^{N}$ for $p[x(0:t)|y(0:t)]$, such that the estimation of quantities of interest at time t can be calculated. The sequential Monte Carlo scheme is to generate a sample $x_i(t)$ and append it to $x_i(0:t_{k-1})$ to form $x_i(0:t)$, and update the weight $w_i(t_{k-1})$ to $w_i(t)$.

If the importance function $q[x(0:t)|y(0:t)]$ can be factorized as

$$q[x(0:t)|y(0:t)] = q[x(t)|x(0:t_{k-1}), y(0:t)] \times q[x(0:t_{k-1})|y(0:t_{k-1})], \tag{33}$$

and $x_i(t)$ is sampled from $q[x(t)|x_i(0:t_{k-1}), y(0:t)]$, the weight of the trajectory $x_i(0:t)$ is

$$\begin{aligned} w_i(t) &\propto \frac{p[x_i(0:t)|y(0:t)]}{q[x_i(0:t)|y(0:t)]} = \frac{p[y(t)|x_i(t)]p[x_i(t)|x_i(t_{k-1})]}{q[x_i(t)|x_i(0:t_{k-1}), y(0:t)]p[y(t)|y(0:t_{k-1})]} \times \frac{p[x_i(0:t_{k-1})|y(0:t_{k-1})]}{q[x_i(0:t_{k-1})|y(0:t_{k-1})]} \\ &\propto \frac{p[y(t)|x_i(t)]p[x_i(t)|x_i(t_{k-1})]}{q[x_i(t)|x_i(0:t_{k-1}), y(0:t)]} w_i(t_{k-1}), \end{aligned}$$

where $p[y(t)|y(0:t_{k-1})]$ is omitted since it is common to all samples. A convenient choice for the importance density is the following *prior importance density* [63, 64]: $q[x(t)|x_i(0:t_{k-1}), y(0:t)] = p[x(t)|x_i(t_{k-1})]$, with which the weight updating equation becomes

$$w_i(t) \propto w_i(t_{k-1}) p[y(t)|x_i(t)], \tag{34}$$

and the posterior filtered density $p[x(t)|y(0:t)]$ can be approximated as

$$p[x(t)|y(0:t)] \simeq \sum_{i=1}^{N} w_i(t) \delta[x(t) - x_i(t)]. \tag{35}$$

From a numerical point of view, the above analysis can be implemented as follows. First generate N samples $\{x_i(0)|i = 1, \cdots, N\}$ from the distribution of $y(0)$ as given in Eq. (30). Each sample has a weight of $1/N$. Each sample $x_i(0)$ then evolves according to the dynamical equation (29) by considering the noise v to get the value at time t_1, e.g. $x_i(t_1)$, and the weights are updated via Eq. (34). The estimation of the state at time t_1 is $\langle x(t_1) \rangle = \sum_{i=1}^{N} w_i(t_1) x_i(t_1)$. During the evolution, it may occur that there are disproportionally fewer

samples about x_i than determined by weight w_i. To avoid this, a sample importance resampling procedure [63] can be applied. That is, we can generate a new set of samples $\{x_i^*,\ w_i^*\}_{i=1}^N$ from the samples $\{x_i,\ w_i\}_{i=1}^N$ with probability being their weights, i.e. each time, the probability to draw sample x_i is its weight w_i (note that the weights are normalized that $\sum_i w_i = 1$). The weights w_i^* for the new samples are then set as $1/N$. As a result of this resampling procedure, the weight w_i of a sample is represented by the number of duplications of the sample, thus the statistics of the samples, e.g. mean value, covariance, etc., are unchanged in the large N limit. The resampling step automatically concentrates the samples in regions of interest and effectively discards samples with low weight. However, this may result in overlaps for some samples. For example, if one sample has a very large weight, after resampling, it may have many duplications, which leads to a degeneration problem. To overcome this difficulty, a regularization process can be applied: A small random vector is added to each sample as a perturbation: $x_i \leftarrow x_i^* + hD\epsilon_i$, where ϵ_i follows the standard normal distribution, D is such that $DD^T = S$ (D^T is the transpose of D). The matrix S is the empirical covariance matrix of the samples before resampling, and the quantity h is a regularization parameter [63, 70]. The samples again propagate via the dynamical equation (29) to yield the values at next time step. The process continues until a desired time span for estimation is reached.

3.3.3 Noise dependence of estimation error

When noise of the system is stationary, i.e. the covariance matrices Σ_v and Σ_e for the process noises v and e in Eqs. (29) and (30) are constant in time, the samples can evolve into a "steady" state and their covariance matrix can be obtained, which is proportional to the estimation error. Suppose at time t_{k-1} the covariance matrix of the samples is $\Sigma_x(t_{k-1})$, which is unknown. Since the dynamical equation f is known, after propagating through Eq. (29), the covariance matrix Σ_f of the samples at time t_k can be expressed in terms of $\Sigma_x(t_{k-1})$ and Σ_v, which reads $\Sigma_f(\Sigma_x(t_{k-1}), \Sigma_v)$. To make use of the correction step [Eq. (32)], we solve x from Eq. (30): $x = g^{-1}(y, e)$. Therefore, for a given observation $y(t)$, the covariance matrix for $x(t)$, from the observational point of view, can be obtained as $\Sigma_s[y(t), \Sigma_e]$. Usually, Σ_s depends mainly on Σ_e, and has little dependence on $y(t)$, thus Σ_s is merely constant in time and can be calculated using the initial observation $y(0)$. The correction procedure is equivalent to a modulation posted by a distribution with covariance matrix Σ_s on a distribution with covariance matrix Σ_f. Suppose both distributions are Gaussian, the resulting distribution is also Gaussian but with covariance matrix $\{\Sigma_f^{-1} + \Sigma_s^{-1}\}^{-1}$. The resampling step does not change the covariance matrix, and the regularization step simply adds a factor of $1 + h^2$. Thus we have $\Sigma_x(t) = \{[\Sigma_f^{-1} + \Sigma_s^{-1}\}^{-1}(1 + h^2)$. In the steady state, we have $\Sigma_x(t) \simeq \Sigma_x(t_{k-1})$, leading to the following self-consistent equation:

$$\Sigma_f^{-1} + \Sigma_s^{-1} = (1 + h^2)\Sigma_x^{-1}, \tag{36}$$

which determines the covariance matrix of the samples, or the posterior pdf $p[x(t)|y(0:t)]$, for given dynamical and observational noise levels. Note that Σ_f is a function of Σ_x and Σ_v. For certain cases, Σ_f can be expressed explicitly in terms of Σ_x and Σ_v, which can be used to further simplify the above equation. For example, for linear dynamical systems, $f = \sqrt{a}x + \sqrt{b}v$, $\Sigma_f = a\Sigma_x + b\Sigma_v$, Eq. (36) becomes:

$$(a\Sigma_x + b\Sigma_v)^{-1} + \Sigma_s^{-1} = (1 + h^2)\Sigma_x^{-1}, \tag{37}$$

From Eq. (36), the dependence of Σ_x on Σ_v and Σ_e can be obtained, which can be used to identify the "leading term" of the noise source, i.e., which noise term has the most influence on Σ_x, and therefore on the estimation precision. This information can be useful for improving the estimation precision by suppressing the leading noise source. In practice, due to the nonlinearity of function g, an explicit expression of Σ_s is not always possible, and a Monte Carlo scheme is viable, i.e., draw a set of samples $\{e_i\}$ from the distribution of e [Eq. (30)]; for each sample e_i, calculate x_i as $x_i = g^{-1}(y(0), e_i)$, then Σ_s can be approximated by the covariance matrix of the samples $\{x_i\}$.

3.3.4 Robust sequential Monte-Carlo scheme for mitigating outliers

The above scheme of sequential Monte-Carlo simulation works well for stationary noise. In the presence of nonstationary disturbances, e.g., outliers, the weight-updating scheme needs to be improved. To be concrete, we treat outliers in the observation, which can lead to a larger covariance matrix Σ_s. This will cause a larger estimation error [Eq. (36)]. Thus, if the outliers can be detected and then discarded, the elements of the covariance matrix of the observations can be reduced. Our idea is to first calculate the empirical distribution of the Monte-Carlo samples, and then compare the observation with this distribution. If the prediction of the observation is close to the center of the samples, the observation is likely to be true and it should be accounted for in the estimation of the state. However, if the prediction deviates from the center of the samples, it is less reliable and should therefore be counted less [71]. Quantitatively, it is convenient to introduce a contribution factor α to characterize this effect. Let $\widetilde{w}_i(t) = w_i(t_{k-1})p[y(t)|x_i(t)]$. We modify Eq. (34) as

$$w_i(t) = (1-\alpha)w_i(t_{k-1}) + \alpha\widetilde{w}_i(t)/\sum_j \widetilde{w}_j(t). \tag{38}$$

Generally, the optimal value of α depends on the distribution of the samples and on the prediction of the observation in a sophisticated way. Our strategy for choosing α is the following. After propagating the samples through the dynamical equation, we calculate Σ_x. The covariance matrix Σ_v of the dynamical noise and Σ_e of the observational noise are assumed to be known. Define $\beta \equiv \sqrt{Tr(\Sigma_v)/Tr(\Sigma_e)}$, $\Delta x \equiv (x_{LS} - \langle x\rangle)/\sqrt{Tr(\Sigma_x)}$, where $\langle x\rangle$ is the average of the samples, and x_{LS} is the least-squares estimation of the state, which minimizes the square error of the observations (this is the case when the number of observations is more than the number of unknowns) [72]. We propose the following criterion for choosing α:

$$\alpha = \begin{cases} 1, & \|\Delta x\| \le c_0, \\ (1-\beta)\frac{c_0}{\|\Delta x\|}(\frac{c_1-\|\Delta x\|}{c_1-c_0})^2 + \beta, & c_0 < \|\Delta x\| \le c_1, \\ \beta\frac{c_1}{\|\Delta x\|}(\frac{c_2-\|\Delta x\|}{c_2-c_1})^2, & c_1 < \|\Delta x\| \le c_2, \\ 0, & c_2 < \|\Delta x\|, \end{cases}$$

where $c_0 \sim 1$, $c_1 \sim 3.5$, $c_2 \sim 7$, and the optimal values can vary for different situations. Note that $\|\Delta x\|$ is the distance between the estimation x_{LS} obtained from the observations and the mean value of the samples $\langle x\rangle$, normalized by the "standard deviation." If $\|\Delta x\| < 1$, the estimation is within the range of the standard deviation and is reliable. If $\|\Delta x\|$ is in the range of one standard deviation to three standard deviations, the observation is less reliable. Since there is noise in the dynamics, the samples may themselves contain some error. The quantity β is introduced to account for such uncertainties. If $\|\Delta x\|$ is even larger, the weight for the observation decreases, and at a certain point, say, beyond seven standard deviations, the observation is deemed as outliers and the weight α is set to be zero.

3.3.5 Numerical support

To substantiate our ideas, we considered a synthetic two-dimensional GPS positioning problem of moving object, say a car, by using GPS observations (see Fig. 14). The origin is the center of the Earth, and the car is originally located at the surface of the Earth—$(0,\ R_e)$ in an Earth centered coordinate, where $R_e = 6357$ km is the radius of the Earth—which is assumed to be unknown. The velocity can be read from the velocimeter, and has a constant true value of 70 mph, or 31.3 m/s. The velocity is assumed to have a Gaussian measurement error with covariance matrix $\Sigma_v = \sigma_v^2\ diag[1\ \ 1]$, where σ_v is regarded as an adjustable parameter. The direction of the velocity changes in time. The car is equipped with a GPS receiver. Four visible satellites ($n_s = 4$) are located at the altitude of 20200 km above the Earth surface with initial angles $\pi/5,\ 7\pi/24,\ 4\pi/7,\ 2\pi/3$ (in the Earth centered coordinate). The satellites orbit the Earth at a period of 12 hours. The receiver on the car can receive GPS signal from each satellite at the frequency of 1 Hz ($\Delta t = t_k - t_{k-1} = 1$ s), from which the distances from

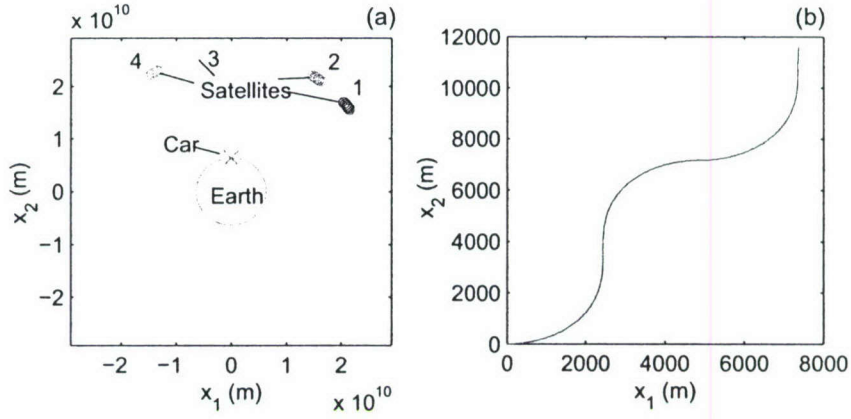

Figure 14: Setup of the numerical problem. (a) The tracks of the satellites and the car for the simulation time (500 seconds). The satellites move counterclockwise. (b) The track of the car, where the origin is shifted to the original position of the car.

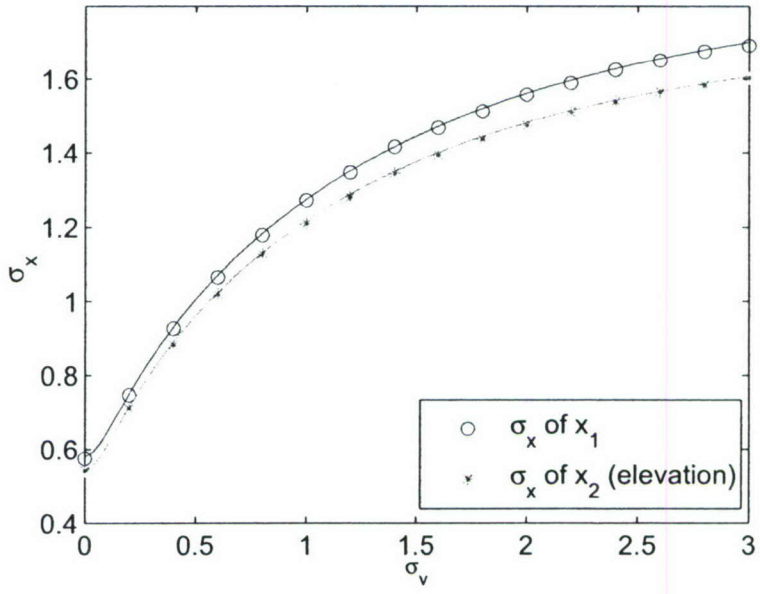

Figure 15: For the two-dimensional positioning problem, dependence of the standard deviations of the samples σ_x for the two coordinates on the standard deviation of the velocity σ_v. The standard deviation of the pseudoranges is $\sigma_p = 2.5$, the number of samples is $N = 1000$, and $h = 0.3$. Symbols are obtained from numeric simulations, where each data is the average of 10 runs, and 100 different time steps for each run are used. The curves are from the our theoretical prediction Eq. (37).

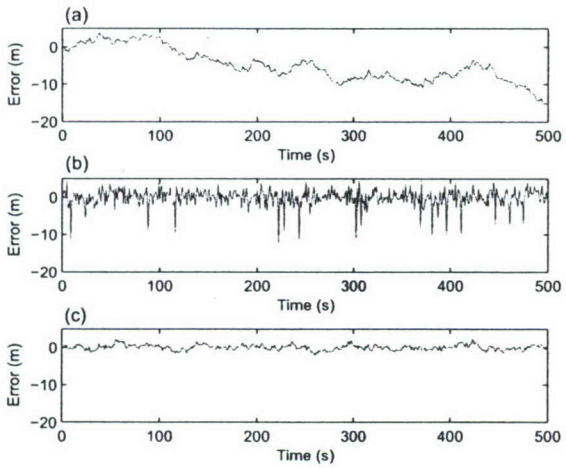

Figure 16: A comparison of the errors of the first coordinate x_1 of the position prediction by velocity information only (a), by least squares of GPS distances with outliers only (b), and by our strategy (c). The parameter values used in the simulation are $\sigma_v = 0.5$, $\sigma_p = 2.5$, $c_0 = 0.7$, $c_1 = 4.2$, $c_2 = 7$, $N = 1000$, and $h = 0.3$.

the satellites to the car P^k (pseudoranges) can be measured. Assuming that the receiver has no clock offset and the satellites are not correlated, we can write the covariance matrix of the pseudoranges as $\Sigma_p = \sigma_p^2 \, I_{n_s}$, where I_{n_s} is the identity matrix of order n_s. A motion model which is linear in the state dynamics and nonlinear in the measurements is [59]

$$x(t) = x(t_{k-1}) + v(t_{k-1}) \cdot \Delta t,$$
$$y(t) = g[x(t)] + e_p(t),$$

where y is the pseudorange measurements $y = [P^1 \;\; P^2 \;\; \cdots \;\; P^{n_s}]^T$. The measurement function is $g(x) = [R^1 \;\; R^2 \;\; \cdots \;\; R^{n_s}]^T$, where $R^j = \|X^j - x\|$ is the Euclidean distance from the car's position x to the j'th satellite X^j, and e_p is the pseudorange observational noise. The covariance matrices for v and e_p are Σ_v and Σ_p respectively.

Figure 15 shows the dependence of Σ_x on Σ_v when Σ_s is given, which can be obtained numerically from the distribution of the pseudoranges (Σ_p). The symbols are obtained from direct simulations, the curves are from our theory Eq. (37). They agree quite well.

To test the robustness of our Monte-Carlo strategy, we added 15 random outliers of 30 meters to the measured pseudoranges of the second satellite in a time span of 500 seconds with measurement frequency 1 Hz. The result of position estimation is shown in Fig. 16. Three cases are presented for comparison. Figure 16(a) shows the prediction error of x_1 where the initial position is known and the measured velocity has standard deviation $\sigma_v = 0.5$. There is a systematic drift of errors. Figure 16(b) shows the prediction error of the least-squares method [72] if only the measured GPS pseudoranges are available (standard deviation $\sigma_p = 2.5$ for each satellite). Figure 16(c) is the estimation error from our proposed Monte-Carlo strategy, which apparently contains no systematic error and exhibits much smaller statistical errors.

Next, we studied the cases with non-Gaussian noise in the GPS pseudorange observations. This might be the case when the car is moving in a city or in the forests, where GPS signal may be blocked by the buildings or the trees and causes difficulty to distinguish multipath signal from the original signal, which may introduce systematic biases [2]. Furthermore, because of the complexity of the environment, at certain moments the original signal may be unavailable. We assume that the distribution of noise in the pseudoranges consists of two Gaussians

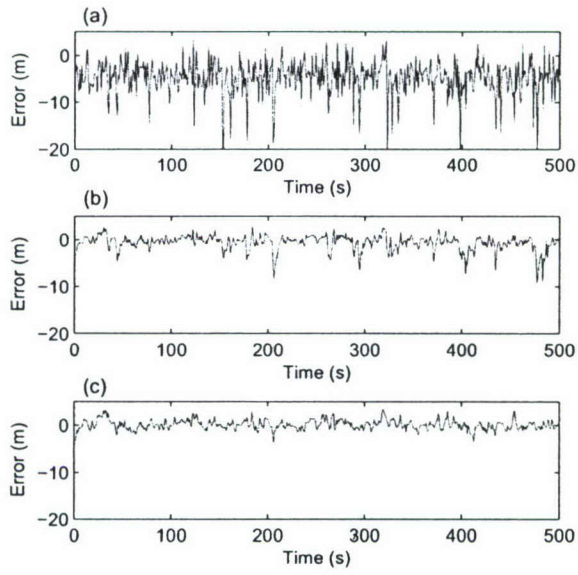

Figure 17: A comparison of the errors of the second coordinate x_2 of the position prediction only by least square of GPS distances with outliers (a), by regularized sequential Monte-Carlo simulation without the robust strategy (b), and by our strategy (c). The parameter values used in the simulation are $\sigma_v = 1$, $\sigma_p = 2.5$, $c_0 = 1.5$, $c_1 = 4.2$, $c_2 = 8$, $N = 1000$, and $h = 0.3$.

with different mean values. The probability density function is:

$$f(x) = b\frac{1}{\sqrt{2\pi}\sigma_1}e^{-\frac{x^2}{2\sigma_1^2}} + (1-b)\frac{1}{\sqrt{2\pi}\sigma_2}e^{-\frac{(x-x_0)^2}{2\sigma_2^2}}, \tag{39}$$

where b is a weight factor and we take $b = 0.6$ in our simulation. Other parameters are $\sigma_1 = \sigma_p = 2.5$, $\sigma_2 = 1$, $x_0 = 8$.

Again, to test the robustness of our algorithm, we added outliers to the GPS pseudorange observations: 20 outliers of 40 meters are added to satellite 2 randomly. Figure 17 compares the errors in position estimation by three methods: the least-squares estimation from the GPS pseudoranges with outliers (a), the estimation by the regularized sequential Monte-Carlo scheme (b), and by our robust sequential Monte-Carlo scheme (c). The least-squares estimation from the pseudoranges has large errors and can have systematic deviations (the average of the error is not zero), as shown in Fig. 17(a). The regularized sequential Monte-Carlo scheme can remove these systematic deviations caused by the non-Gaussian distribution but is affected by the outliers, which can be seen from the spikes in Fig. 17(b). Our robust sequential Monte-Carlo scheme can recover from both the systematic deviations and the outliers [Fig. 17(c)]. In fact, the average absolute value of the errors can be 30% smaller.

The current robust scheme deals with observational outliers. If there are dynamical outliers—e.g. the outliers appear in v—the current scheme needs to be modified to cope with the problem. Observations after such an event will be needed to identify an outlier.

3.3.6 Discussions

In conclusion, we have obtained a self-consistent equation for the estimation precision of the Bayesian inference in terms of the dynamical noise and the observational noise levels. The equation may provide insights into

designing improved sequential Monte-Carlo simulations with higher precision. We also proposed a strategy to deal with sudden, large disturbances that are inevitable in physical observations. The effectiveness of our method has been tested numerically. While we used a standard kinematic GPS positioning problem to demonstrate the working of our approach, it is general and applicable to signal-processing problems where outliers are present and are to be mitigated. Sequential Monte-Carlo simulations have begun to be used widely in various estimation problems in science and engineering. Our contribution provides a robust strategy for improving the estimation precision when experimental observations are nonstationary or even temporally interrupted.

References

[1] D. Kim and R. Langley, Int. Symp. on GPS/GNSS, Seoul, Korea (2000).

[2] B. Hofmann-Wellenhof, H. Lichtenegger, and J. Collins, *Global Positioning System, Theory and Practice*(5th ed. Springer-Verlag, New York, 2001).

[3] C. C. Counselman and S. A. Gourevitch, IEEE Trans. Geoscience and Remote Sensing **GE-19**, 244-252 (1981).

[4] G. C. Xu, pp. 280-283 in *GPS - Theory, Algorithms and Applications* (Springer Heidelberg, 2003).

[5] H. Hatch, Proc. of KIS 90, Canada, 1990)

[6] E. Frei and G. Beutler (1990) Manuscr. Geod. **15**, 325-356 (1990).

[7] P. J. G. Teunissen, LGR Series (Delft Geodetic Computer Centre, 1993).

[8] P. J. G. Teunissen, Proc. IEEE Position, Location and Navigation Symp. (Las Vegas, NV, 1994).

[9] P. J. G. Teunissen, J. Geod. **70**, 65-82 (1995).

[10] P. J. G. Teunissen, J. Geod. **71**, 589-602 (1996).

[11] D. Chen and G. Lachapelle, Navigation: J. Inst. of Navigation **42** 371-390 (1995).

[12] P. L. Xu, E. Cannon, and G. Lachapelle Proc. IUGG95 Assembly (Boulder, 2-14 July, 1995).

[13] P. L. Xu J. Geod. Soc. Jpn. **44**, 169-187 (1998).

[14] P. L. Xu J. Geod. **75**, 408-423 (2001).

[15] Z. Li and Y. Gao, Geomatica **52**, 433-439 (1998).

[16] A. Hassibi and S. Boyd, IEEE Trans. Signal Processing **46**, 2938-2952 (1998).

[17] B. Azimi-Sadjadi and P. S. Krishnaprasad Proc. Ame. Control Conf. **5**, 3761-3766 (2001).

[18] P. L. Xu IEEE Trans. Information Theory **52**, 3122-3138 (2006).

[19] G. C. Xu, A general criterion of integer ambiguity search. J. of Global Positioning Sys. **1**, 122-131 (2002).

[20] M. Wei M and K. P. Schwarz Proc. of ION GPS-95 (Palm Springs, CA, 1995).

[21] Z. Li, Proc. of ION GPS-95 (Palm Springs, CA, 1995).

[22] M. Amin, IEEE Trans. Signal Processing **45**, 90-102 (1997).

[23] M. Amin, R. Ramineni, and A. Lindsey, Proc. of the 33rd ASILOMAR conference (Monterey, CA, 1999).

[24] R. Fante and J. J. Vaccaro, IEEE Trans. Aerospace Elec. Sys. **36**, 549-564 (2000).

[25] G. V. Tsoulos, *Adaptive Antennas for Wireless Communications* (IEEE Press, Piscataway, NJ, 2001).

[26] G. C. Xu, MFGsoft - Multi-functional GPS/(Galileo) software – Software User Manual (Version of 2004), Scientific Technical Report STR04/17 of GeoForschungsZentrum (GFZ) Potsdam, ISSN 1610-0956 (2004).

[27] S. Haykin, *Communication Systems* (4th ed. Wiley, New York, 2001).

[28] N. E. Huang, Z. Shen S. F. Long, M. C. Wu, and H. H. Shih, Proc. R. Soc. A **454**, 903-995 (1998).

[29] J. B. Y. Tsui, *Fundamentals of GPS Receivers: A Software Approach* (2nd Ed, John Wiley and Sons, New York, 2005).

[30] M. J. McKeown, R. Saab, and R. Abu-Gharbieh, pp. 679-682 in Neural Engineering, Conference Proceedings. 2nd International IEEE EMBS Conference (March, 2005).

[31] R. Balocchi, D. Menicucci, and M. Varanini, Proceedings of the 25th Annual Intemational Conference of the IEEE EMBS (Cancun, Mexico, September, 2003).

[32] J. W. Ketchum and J. G. Proakis, IEEE Trans. Comm. **COM-30**, 913-924 (1982).

[33] L. B. Milstein, Proc. IEEE **76**, 657–671 (1988).

[34] B. Badke and A. Spanias, Proc. of IEEE Conf. Acoustics, Speech, and Signal Processing (May 2002).

[35] P. T. Capozza, B. J. Holland, T. M. Hopkinson, and R. L. Landrau, IEEE J. Solid State Circuits **35**, 401-411 (2000).

[36] W. L. Myrick, J. S. Goldstein, and M. D. Zoltowski, Proc. IEEE Inter. Conf. Acoustic, Speech, and Signal Processing **4**, 2233-2236 (2001).

[37] M. G. Amin, R. S. Ramineni, and A. R. Lindsey, Proc. of the 33rd ASILOMAR conference (Monterey, CA, Oct. 1999).

[38] R. A. Iltis, IEEE Trans. Comm. **38**, 1677-1685 (1990).

[39] S. J. Kim and R. A. Iltis, Proc. of Conf. Information Sciences and Systems (Princeton University, March 20-22, 2002).

[40] T. Yalcinkaya and Y.-C. Lai, Phys. Rev. Lett. **79**, 3885-3888 (1997).

[41] Y.-C. Lai, Phys. Rev. E **58**, R6911-R6914 (1998).

[42] D. G. Duffy, J. Atmos. Oceanic Tech. **21**, 599-611 (2004).

[43] A. Mansour, A. K. Barros, and N. Ohnishi, IEICE Trans. Funda. Electronics, Commun. Comp. Sci. **E83-A**, 1498-1512 (2000).

[44] K. Anand, G. Mathew, and V. U. Reddy, IEEE Sig. Proc. Lett. 176-178 (Sept. 1995).

[45] E. Chaumette, P. Comon, and D. Muller, IEE Proc. Part F **140**, 395-401 (1993).

[46] D. L. Lathauwer, D. B. Moor, and J. Vandewalle J, pp. 134-138 in Proc. of IEEE Sig. Proc./Athos Workshop on Higher-Order Statistics (Girona, Spain, Jun. 1995).

[47] D. T. Pham, IEEE Trans. Sig. Proc. **44**, 2768-2779 (1996).

[48] A. Silberfarb, P. S. Jessen, and I. H. Deutsch, Phys. Rev. Lett. **95**, 030402 (2005).

[49] E. Bagan, M. A. Ballester, R. Muñoz-Tapia, and O. Romero-Isart, Phys. Rev. Lett. **95**, 110504 (2005).

[50] J. P. M. Heald and J. Stark, Phys. Rev. Lett. **84**, 2366 (2000).

[51] R. Meyer and N. Christensen, Phys. Rev. E **65**, 016206 (2001).

[52] P. Crotty, J. García-Bellido, J. Lesgourgues, and A. Riazuelo, Phys. Rev. Lett. **91**, 171301 (2003).

[53] M. Wyman, L. Pogosian, and I. Wasserman, Phys. Rev. D **72**, 023513 (2005).

[54] N. Christensen and R. Meyer, Phys. Rev. D **64**, 022001 (2001).

[55] N. J. Cornish and J. Crowder, Phys. Rev. D **72**, 043005 (2005).

[56] W. Rieping, M. Habeck, and M. Nilges, Science **309**, 303 (2005).

[57] V. Baldazzi, S. Cocco, E. Marinari, and R. Monasson, Phys. Rev. Lett. **96**, 128102 (2006).

[58] R. Jansen *et al.*, Science **302**, 449 (2003).

[59] F. Gustafsson, F. Gunnarsson, N. Bergman, U. Forssell, J. Jansson, R. Karlsson, and P-J. Nordlund, IEEE Trans. on Signal Processing **50**, 425 (2002).

[60] E. T. Jaynes, edited by G. L. Bretthorst, *Probability theory: the logic of science* (Cambridge University Press, New York, 2003).

[61] W. Gilks, S. Richardson, and D. Spiegelhalter, *Markov Chain Monte Carlo in practice* (Chapman & Hall, 1996).

[62] A. Doucet, N. de Freitas, N. Gordon, editors, *Sequential Monte Carlo methods in practice* (Springer Verlag, New York, 2001).

[63] S. Arulampalam, S. Maskell, N. Gordon, and T. Clapp, IEEE Trans. on Signal Processing **50**, 174 (2002).

[64] P.M. Djuric, J.H. Kotecha, J. Zhang, Y. Huang, T. Ghirmai, M.F. Bugallo, J. Miguez, IEEE Signal Processing Magazine **20**, Issue 3, 19 (2003).

[65] L. Fahrmeir, R. Künstler, Metrika **49**, 173 (1999).

[66] T. Proietti, Journal of Time Series Analysis **24**, 221 (2003).

[67] A. H. Jazwinsky, *Stochastic Processes and Filtering Theory* (Academic Press: New York, 1970).

[68] E. A. Wan and R. Van der Merwe, in *Kalman Filtering and Neural Networks*, Chapter 7 (Wiley Publishing, 2001).

[69] A. Doucet, S. Godsill, and C. Andrieu, Statistics and Computing **10**, 197 (2000).

[70] C. Musso, N. Oudjane and F. LeGland, in *Sequential Monte Carlo methods in practice*, edited by A. Doucet, N. de Freitas, and N. Gordon (New York, Springer, 2001).

[71] Y. Yang, H. He, and G. Xu, J. Geod. **75**, 109 (2001).

[72] G. Strang and K. Borre, *Linear Algebra, Geodesy, and GPS* (Wellesley-Cambridge Press, Wellesley MA, 1997).

4 Personnel Supported and Theses Supervised by PI

4.1 Personnel Supported

The following people received partial salaries from the AFOSR Project in various time periods.

- **Faculty**: Ying-Cheng Lai (PI), Professor of Electrical Engineering, Affiliated Professor of Physics
- **Graduate Students**

1. Mayur Shah, MS, Electrical Engineering, 2/16/04-7/15/04
2. Suprada Urval, MS, Electrical Engineering, 2/16/04-12/31/04
3. Vinayak Kamath, MS, Electrical Engineering, 5/16/05 - 8/15/06
4. Anusha Rammohan, MS, Electrical Engineering, 5/16/05 - 12/31/06
5. Liang Huang, Ph.D., Electrical Engineering, 8/16/05 - 8/15/07

4.2 Theses supervised by PI as a result of the AFOSR support

1. Mayur Shah, Electrical Engineering, August 2004. Thesis: *Integer ambiguity resolution with GPS signals in jamming environment.*
2. Suprada Urval, Electrical Engineering, May 2005. Thesis: *Antijamming of GPS signals.*
3. Vinayak Kamath, Electrical Engineering, ASU, December 2006. Thesis: *Signal-processing techniques for antijamming with GPS signals and noise reduction in chaotic dynamical systems.*
4. Anusha Rammohan, Electrical Engineering, ASU, May 2007. Thesis: *Integer-ambiguity resolution in global positioning systems using particle filters.*

5 List of Publications

1. M. Shah and Y.-C. Lai, "Performance of integer parameter estimation algorithm for GPS signals in noisy environment," pp. 166-174 in *ION GNSS 17th International Technical Meeting of the Satellite Division*, Sept. 21-24, 2004, Long Beach, CA.
2. V. Kamath, Y.-C. Lai, S. Urval, and L. Zhu, "Empirical mode decomposition and blind source separation methods for antijamming with GPS signals," pp. 335-341 in IEEE PLANS (Position Location and Navigation Symposium), April 24-26, 2006, San Diego, CA.
3. L. Huang and Y.-C. Lai, "Sequential Monte Carlo scheme for Bayesian estimation in the presence of data outliers," *Physical Review E* **75**, 056705(1-6) (2007).
4. L. Zhu, Y.-C. Lai, M. Shah, and S. Mahmood "Efficiency of carrier-phase integer ambiguity resolution for precise GPS positioning in noisy environments," *Journal of Geodesy* **81**, 149-156 (2007).
5. V. Kamath and Y.-C. Lai, "Empirical mode decomposition with applications to noise reduction and antijamming," in preparation.
6. A. Rammohan, L. Huang, and Y.-C. Lai, "Integer ambiguity resolution using particle filters," in preparation.

6 Interactions/Transitions

There was an active collaboration with Drs. S. Mohamod and J. Murchison at Eglin AFB. The activities resulted in one joint paper published in *Journal of Geodesy*.

During the project period, the PI gave two invited talks on GPS, in addition to talks at annual AFOSR Test and Evaluation Workshops.

1. "Performance of integer least-squares method for ambiguity resolution with GPS signals in the presence of noise," Seminar, Tamasek Laboratory and Department of Physics, National University of Singapore, July 20, 2004.

2. "Empirical mode decomposition and application to antijamming with GPS signals," Air Force T&E Days Conference, Nashville, TN, December 8, 2005.

7 Past Honors

1. PECASE, 1997.

2. Election as a Fellow of the American Physical Society, 1999. Citation: *For his many contributions to the fundamentals of nonlinear dynamics and chaos.*